

Accepted Manuscript

Tectono-Stratigraphic evolution of the upper jurassic-neocomian rift succession,
Araripe Basin, Northeast Brazil

Claiton Marlon dos Santos Scherer, Emanuel Ferraz Jardim de Sá, Valéria Centurion
Córdoba, Debora do Carmo Sousa, Mayara Martins Aquino, Fátima Maria Canelas
Cardoso

PII: S0895-9811(13)00151-X

DOI: [10.1016/j.jsames.2013.10.007](https://doi.org/10.1016/j.jsames.2013.10.007)

Reference: SAMES 1226

To appear in: *Journal of South American Earth Sciences*

Received Date: 21 May 2013

Accepted Date: 24 October 2013

Please cite this article as: Scherer, C.M.d.S., Jardim de Sá, E.F., Córdoba, V.C., Sousa, D.d.C., Aquino, M.M., Cardoso, F.M.C., Tectono-Stratigraphic evolution of the upper jurassic-neocomian rift succession, Araripe Basin, Northeast Brazil, *Journal of South American Earth Sciences* (2013), doi: 10.1016/j.jsames.2013.10.007.

This is a PDF file of an unedited manuscript that has been accepted for publication. As a service to our customers we are providing this early version of the manuscript. The manuscript will undergo copyediting, typesetting, and review of the resulting proof before it is published in its final form. Please note that during the production process errors may be discovered which could affect the content, and all legal disclaimers that apply to the journal pertain.



1 **TECTONO-STRATIGRAPHIC EVOLUTION OF THE UPPER JURASSIC-**
2 **NEOCOMIAN RIFT SUCCESSION, ARARIPE BASIN, NORTHEAST BRAZIL**

3
4 Claiton Marlon dos Santos Scherer¹, Emanuel Ferraz Jardim de Sá², Valéria Centurion
5 Córdoba², Debora do Carmo Sousa², Mayara Martins Aquino³, Fátima Maria Canelas
6 Cardoso⁴

7
8 ¹ UFRGS, Instituto de Geociências, P.O. Box 15001, CEP 91501-970, Porto Alegre -
9 RS, Brazil.

10 ² UFRN, Centro de Ciências Exatas e da Terra, Departamento de Geologia,
11 Laboratório de Geologia e Geofísica de Petróleo, Programa de Pós-Graduação em
12 Geodinâmica e Geofísica, Natal-RN, Brazil

13 ³ Petróleo Brasileiro S.A., E&P - EXP/IABS/PN, Rio de Janeiro, Brazil

14 ⁴ Universidade de Coimbra, Centro de Geociências, Ciências da Terra FCTUC,
15 Coimbra, Portugal

16
17 E-mail addresses: claiton.scherer@ufrgs.br (C.M.S. Scherer), emanuel@ccet.ufrn.br
18 (E.F. Jardim de Sá), vcordoba@ufrnet.br (V.C.Córdoba), debora@geologia.ufrn.br
19 (D.C. Sousa), Mayara_aquino@petrobras.com.br (M.M. Aquino),
20 fatima.cardoso18@hotmail.com (F.M.C. Cardoso)..

21
22 **Abstract**

23 The rift succession of the Araripe Basin can be subdivided into four depositional
24 sequences, bounded by regional unconformities, which record different
25 palaeogeographic and palaeoenvironmental contexts. Sequence I, equivalent to the
26 Brejo Santo Formation, is composed of fluvial sheetflood and floodplain facies
27 association, while Sequence II, correspondent to the lower portion of the Missão Velha
28 Formation, is characterised by braided fluvial channel belt deposits. The fluvial deposits
29 of Sequences I and II show palaeocurrents toward SE. The Sequence III,
30 correspondent to the upper portion of Missão Velha Formation, is composed of fluvial
31 sheetflood deposits, which are overlain by braided fluvial channel deposits displaying a
32 palaeocurrent pattern predominantly toward SW to NW. Sequence IV, equivalent to the
33 Abaiara Formation, is composed of fluvio-deltaic-lacustrine strata with polymodal
34 paleocurrent pattern. The type of depositional systems, the palaeocurrent pattern and
35 the comparison with general tectono-stratigraphic rift models led to the identification of
36 different evolutionary stages of the Araripe Basin. Sequences I, II and III represent the
37 record of a larger basin associated to an early rift stage. However, the difference of the

38 fluvial palaeocurrent between sequences II and III marks a regional rearrangement of
39 the drainage system related to tectonic activity that compartmentalised the large
40 endorheic basin, defining more localised drainage basins separated by internal highs.
41 Sequence IV is associated with the renewal of the landscape and implantation of half-
42 graben systems. The high dispersion of palaeocurrents trends indicate that
43 sedimentary influx occurs from different sectors of the half-grabens.

44

45 **Keywords**

46 Araripe Basin, Rift Basin, Continental Sequence Stratigraphy, Continental Depositional
47 Systems

48

49 **1. Introduction**

50

51 In recent years, numerous studies have addressed the tectonic-stratigraphic
52 evolution of the rift basin, focusing on the influence of the tectonic on basin geometry
53 and on accommodation and sediment supply ratio (A/S ratio) during the different
54 stages of rifting (Prosser, 1993; Bosence, 1998; Galthorper and Leeder, 2000; Morley,
55 2002; Kuchle & Scherer, 2010). However, there are few studies detailing the facies
56 architecture and depositional dynamics associated with each of the evolutionary stages
57 of rifting, especially with regard to the initial stages of rifting, where depocenters are
58 difficult to identify and fill patterns are diverse and yet poorly understood (Kinabo et al.,
59 2007; Morley, 2002; Kuchle et al., 2011).

60 The sedimentary deposits of the Araripe Basin cover an area larger than 9,000 km²,
61 consisting of one of more extensive interior basins of the Brazilian Northeast (Figure 1).
62 As with the other interior basins, the origins of Araripe Basin are linked to the rifting and
63 opening processes of the South Atlantic (Ghignone et al., 1986; Assine, 2007).
64 Geometry and evolution of these basins are strongly conditioned by structures of the
65 Precambrian/Neopalaeozoic basement, whose reactivation controlled the arrangement
66 of depocenters over time. The Mesozoic stratigraphic record of the Araripe Basin
67 reflects different stages of subsidence related to three main phases (Ponte and Ponte
68 Filho, 1996): (a) the "Pre-Rift" phase, characterised by regional subsidence produced
69 by visco-elastic lithospheric stretching; b) the Rift phase, with accentuated mechanical
70 subsidence, forming graben and/or half-graben systems; and c) the Post-Rift phase,
71 characterised by the predominance of thermal subsidence. The main objective of this
72 paper is to detail the stratigraphic architecture of the section corresponding to "pre-rift"
73 and rift phases, aiming at understanding the depositional geometry, the fill patterns and
74 main controls on sedimentation and accumulation of different evolutionary stages of

75 rifting. Its specific goals include: (1) to identify and correlate unconformities that permit
76 the recognition of different depositional sequences; (2) to analyze the facies
77 architecture and the palaeocurrent pattern of each of the depositional sequences
78 proposed; and (3) to reconstruct the tectono-sedimentary evolution of the rift succession
79 of the Araripe Basin. These results were obtained as part of a project intitled Interior
80 Basins of the Northeast (*Bacias Interiores do Nordeste*) (PETROBRAS/UFRN/PPGG),
81 whose preliminary results were presented in graduate MSc (Garcia, 2009, Aquino,
82 2009; Cardoso, 2010; Costa 2012) and at scientific meetings (Jardim de Sá et al.,
83 2009, 2010, 2011, Cardoso et al., 2009, 2010).

84 To reach these objectives, 5 stratigraphic sections, each 5 to 90 m thick, were
85 measured and analysed in detail (Fig. 1). High-resolution sedimentary logs were
86 measured in order to define the main sedimentary elements of the studied interval. In
87 addition to detailed facies analysis of logged sections, architectural panels were made
88 to define the two-dimensional (2D) geometries of the deposits. Facies were defined
89 mainly on the basis of grain-size and sedimentary structures. Palaeocurrent
90 orientations were measured from cross-stratified beds. Paleocurrent readings were
91 corrected to the horizontal surface based on the S_0 depositional surface (Tucker,
92 1996). Unconformities surfaces were identified within the main outcrops and correlated
93 between sedimentary logs (the sections), allowing the individualisation of different
94 depositional sequences.

95

96 **2. Regional Stratigraphic Framework**

97 The Araripe Basin, similar to other basins that occur in the interior of Northeast
98 Brazil, is associated with the Neocomian rift event that resulted in the separation of the
99 South American and African continents, specifically, in the opening of the East
100 Brazilian continental margin (Ghignone et al., 1986; Assine, 2007). Geometry and
101 evolution of these basins are strongly conditioned by structures of the
102 Precambrian/Neopalaeozoic basement, whose reactivation controlled the arrangement
103 of depocenters over time. As discussed by Ponte and Appi (1990), Chang *et al.* (1992),
104 Matos (1992,1999) and other authors, this event included a range of onshore aborted
105 rift basins, which extend from Recôncavo-Tucano-Jatobá grabens system to the
106 Potiguar graben, all of which were controlled by a principal NW extension. Alternative
107 models have been proposed by other authors (e.g., Françolin *et al.* 1994), though the
108 kinematics of the NW extension is supported by recent studies (Córdoba et al. 2008;
109 Aquino, 2009; Cardoso, 2010; Jardim de Sá et al. 2010, 2011).

110 In the case of the Araripe Basin, the tectonic rift affected the Precambrian
111 granite-gneiss and Paleozoic sedimentary basements. Studies by Matos (1992, 1999),
112 Aquino (2009) and Cardoso (2010) describe half-grabens controlled by normal faults in
113 the NE direction that are commonly tilted to the SE and associated with strike slip faults
114 that define a conjugate pair (E-W sinistral and NE dextral), which also agrees with the
115 NW distension.

116 According to the studies by Ponte and Appi (1990), Assine (1990, 1992) and
117 Ponte and Ponte Filho (1996), the Araripe Basin may be subdivided into sequences
118 bound by regional unconformities that reflect distinct tectonic stages in the basin.
119 Assine (2007) integrated these different proposals, identifying four large units limited by
120 unconformities: (1) the Palaeozoic Sequence, represented by the alluvial sedimentation
121 of the Mauriti Formation and interpreted as the residual deposits of a large intracratonic
122 basin; (2) the Pre-Rift Supersequence (Neojurassic), corresponding to the Brejo Santo
123 and Missão Velha formations; (3) the Rift Supersequence (Neocomian), equivalent to
124 the Abaiara Formation; and (4) the Post-Rift Supersequence. The latter may be
125 subdivided into two higher-frequency sequences: (a) Post-Rift Sequence I (Aptian-
126 Albian), corresponding to the Barbalha and Santana formations; and (b) Post-Rift
127 Sequence II, equivalent to the Araripina and Exu formations.

128 The interval analysed in the present study includes the pre-rift and rift
129 supersequences of the Araripe Basin, corresponding to the Brejo Santo, Missão Velha
130 and Abaiara formations, which are grouped in the Cariri Valley Group (Grupo Vale do
131 Cariri) (Ponte and Appi, 1990; Assine, 2007) (Table 1). The Brejo Santo Formation is
132 predominantly made up of red, or more rarely green mudstones, rich in ostracod
133 fossils. Sometimes, intercalated layers of fine grained sandstones are observed, mainly
134 toward the top of the unit (Assine, 1990). The Brejo Santo Formation is interpreted as
135 deposits of the shallow, broad and ephemeral lakes (Assine, 1990). The Missão Velha
136 Formation is compound by fine to very coarse-grained sandstones, sometimes
137 containing fossil trunks, intercalated with rare and discontinuous mudstones lenses.
138 The Missão Velha Formation has been interpreted as braided fluvial channels deposits
139 with a regional palaeoflow toward the SE (Assine, 1994). Finally, the Abaiara
140 Formation is characterized by different litological types with a predominance of fine to
141 medium-grained sandstones and mudstones. This unit has been interpreted as
142 deposits of fluvial, deltaic and lacustrine depositional systems. According to Assine
143 (1994), the fluvial and deltaic deposits of the Abaiara Formation show paleocurrents
144 toward the SE.

145 In the present study, the stratigraphic data are presented and interpreted
146 according to the commonly accepted hypothesis, in which the Brejo Santo Formation

147 was deposited during the Neojurassic (Dom João Stage) (Coimbra et al., 2002, Assine,
148 2007). Meanwhile, 100 miles north of Araripe Basin are described reddish mudstones
149 (Lavras da Mangabeira Formation) that are intruded by basic dikes aged of 185 Ma, as
150 discussed by Jardim de Sá et al. (2010, 2011). The mudstones of the Lavras da
151 Mangabeira Formation overly paleozoic sandstones, defining a stratigraphic context
152 very similar to Brejo Santo Formation. As a result, Jardim de Sá (2010, 2011) raise the
153 possibility that the lower part of the Brejo Santo Formation may be older than
154 Neojurassic.

155

156 **3. Sequence Stratigraphy of the Jurassic-Neocomian Succession**

157

158 The Upper Jurassic-Neocomian section of Araripe Basin can be subdivided into four
159 depositional sequences. These sequences are designated, from the base to the top, as
160 Sequences I, II, III and IV (Figure 2). The criteria used to identify unconformities in
161 outcrops include: (1) an abrupt facies change, which may involve both a change in the
162 depositional systems or modification of facies architecture within a specific depositional
163 system; (2) an abrupt change in the texture and grain size across the unconformity;
164 and (3) changes in the palaeocurrent patterns. The lithofacies description for each
165 depositional sequence is shown in Table 1 and is based on the original table from Miall
166 (1977).

167

168 **3.1 Sequence I**

169 Sequence I corresponds entirely to the Brejo Santo Formation. This sequence displays
170 a thickness of approximately 400 m (Ponte and Appi, 1990; Assine, 1992). The lower
171 and the upper boundaries of Sequence I comprise regional scale unconformities with
172 the Mauriti and Missão Velha formations, respectively (Figure 2). Sequence I is
173 composed of two distinct facies associations (Figure 3): (1) Fluvial Sheetflood Facies
174 Association and (2) the Floodplain Facies Association.

175

176 *3.1.1 Fluvial Sheetflood Facies Association*

177 This facies association is characterised by fine to medium-grained sandstones,
178 arranged in 1-5 m thick tabular bodies, that can be traced laterally more than 80 m
179 (maximum outcrop extent). Fining-upward trends are common, with the tops of the
180 cycles grading to mudstones of the floodplain facies association. The tabular bodies
181 are bounded at the base by flat or slightly erosional surfaces that may eventually be
182 marked by < 10cm thick lags of mud and carbonate intraclasts (Figure 3). Internally,

183 sandstone bodies can be composed of a single lithofacies (Sm) or a succession of the
184 different lithofacies. In the latter case, the sandbodies are characterized at the base by
185 massive (Sm), low-angle (Sl) and/or horizontal (Sh) laminated sandstones, which are
186 succeeded by ripple cross-laminated sandstones (Sr). Trough cross-bedding
187 sandstones (St) are isolated and rare (Figure 3). Measurements of the direction of the
188 dip of the cross-strata display a unimodal pattern with a mean vector toward the SE
189 (Figures 2 and 3).

190 The tabular bodies can be interpreted as the result of flash flood deposition in
191 laterally extensive, unconfined sheets or poorly confined fluvial channels. The
192 abundance of massive, low-angle or horizontally stratified sandstones suggests that
193 flow events were short lived and of high intensity (Tunbridge, 1984; Hampton and
194 Horton, 2007). The intercalation of these lithofacies within the same succession
195 indicates variations in the concentration of sediments and in the flow velocity. The
196 massive sandstones are the result of hyperconcentrated flows in which the
197 concentration of sandy sediment in suspension inhibits the turbulence and separation
198 of the flow, which are necessary for the embryonation of dunes (Allen and Leeder,
199 1980). The sediment is deposited *en masse* during the deceleration of the flow. In turn,
200 the low-angle and horizontal stratified sandstones indicate more diluted flow conditions
201 in which the sediments are predominantly transported by traction in high-flow regime
202 (Allen and Leeder, 1980). The occurrence of ripple cross stratified sandstone in the
203 upper portion of the tabular bodies is the result of waning flow velocity associated with
204 flow termination or channel abandonment (Miall, 1996). Intraformational lags at the
205 base of sheet sandstone bodies represent the reworking of deposits accumulated in
206 the floodplain areas.

207

208 3.1.2 Distal Floodplain Facies Association

209 This facies association is characterized by up to 5 m thickness reddish
210 mudstones intercalated occasionally with tabular sandstones (Figure 3). Mudstones are
211 massive, with ostracod fossils, sometimes exhibiting layers of calcareous concretions.
212 Sandstones are fine to medium-grained, well-sorted and deposited in tabular layers, 10
213 to 30 cm thickness, with planar and non-erosive basal contact. The sandstones
214 commonly display ripple cross-lamination (Sr). Sometimes, horizontal lamination (Sh)
215 can be observed.

216 This facies association is interpreted as floodplain deposits, which may
217 represent two distinct depositional contexts: (a) overbank flooding resulting from
218 unconfined flow originating from overtopped channels when they occur adjacent to

219 lenticular sandbodies; or (ii) downslope, unconfined sedimentation associated with
220 terminal flooding stages (Hampton and Horton, 2007; Spalletti and Piñol, 2005).
221 Tabular sandstone beds composed of horizontal lamination and ripples cross-
222 laminated are interpreted as the products of poorly developed traction currents during
223 the waning stages of flood events (Hampton and Horton, 2007). Mudstones, in turn,
224 must have been deposited by the gravitational settling of the particles in suspension
225 during the final stages of flooding or in temporary lacustrine bodies that form on the
226 alluvial plain. The levels characterised by carbonate nodules are interpreted as
227 calcareous palaeosols (Ray and Chakraborty, 2002).

228

229 **3.2 Sequence II**

230

231 Sequence II is equivalent to the lower section of the Missão Velha Formation, bounded
232 at the top and the base by unconformities (Figure 2 and 4). This sequence displays a
233 thickness of between 20 and 30 m and it is composed of two distinct facies association
234 (Figures 4 and 5): (1) Braided Fluvial Channel Belt and (2
235) Overbank Facies Association.

236

237 **3.2.1 Braided Fluvial Channel Belt Facies Association**

238 This facies association consists of fine to very coarse-grained sandstones,
239 moderately sorted, sometimes containing fossil trunks, arranged in sandstones bodies,
240 5 to 15 m thick, that extend laterally for more than 300 m (maximum outcrop extent).
241 The sandstone bodies are bounded at the base by erosive, slightly concave surfaces,
242 which in some cases are marked by concentrations of granules and pebbles. Internally,
243 the sandstone bodies exhibit a weakly developed fining upward pattern. The
244 sandstones exhibit planar (Sp) and trough (St) cross-bedding, arranged in 0.2 to 1 m
245 thick sets (Figures 4 and 5). Horizontal stratification (Sh) and low angle cross-
246 stratification (Sl) sandstones are rare and normally restricted to isolated sets, 10 to 30
247 cm thick. Sometimes, it is possible to identify compound cross-strata, 2 and 3 m thick,
248 which internally display sets of planar and trough cross-bedding bounded by inclined
249 surfaces dipping in the same direction of the cross strata. The dipping of the bounding
250 surfaces varies from 3° to 10° , and those with a lower angle (3° to 5°) are only visible in
251 sections parallel to the dipping direction, where a smooth downlap of these surfaces
252 can be identified over the basal surface of the compound cross-strata. Measurements
253 of the direction of the dip of the cross-strata display a unimodal pattern with a mean
254 vector toward the SE (Figures 2, 4 and 5).

255 The occurrence of sandstone bodies bounded at the base by erosive surfaces
256 outlined by granules and pebbles lags and internally composed of sets of planar and
257 trough cross-strata with a unimodal direction of the palaeocurrents indicate that this
258 facies association represents fluvial channel deposits. The compound cross-strata can
259 be interpreted as macroforms migrating in-channel. The fact that the cross-strata
260 exhibit the same dip direction of the bounding surfaces allows for the conclusion that
261 the compound cross-strata represent downstream accretion macroforms with
262 superimposed, small-scale bedforms (Miall, 1996; Chakraborty, 1999; Jo and Choung,
263 2001). The sandstone bodies sheet geometry, prevailing coarse-grained nature of the
264 deposits, common presence of the downstream macroforms, the weak development of
265 the fining upward succession and the low dispersion of the palaeocurrent data suggest
266 low sinuosity, braided channel belt deposits (Scherer and Lavina, 2006; Miall, 1996).

267

268 3.2.2 Overbank Facies Association

269 This facies association is rare and occurs intercalated with braided fluvial
270 channel-belt deposits, consisting mainly of red massive mudstone (Fm) (Figures 5).
271 Individual bodies are decimetres thick (< 50cm) and extend laterally for less than 30 m,
272 invariably truncated by the overlying sandstone bodies of the braided fluvial channel
273 belt facies association.

274 The fine-grained deposits are interpreted as overbank deposits accumulated
275 through gravitational settling of the suspended load within flooded areas surrounding
276 braided channel belts (Miall, 1996).

277

278 3.3 Sequence III

279

280 Sequence III, 20 to 30 m thick, corresponds lithostratigraphically to the upper
281 portion of the Missão Velha Formation (Fambrini et al., 2011). Due to similarity of the
282 facies association (both are fluvial deposits), it is difficult to identify the unconformity
283 surface between sequences II and III, defining a cryptic sequence boundary
284 (terminology of Miall and Arush, 2001). Among the main criteria used for this
285 identification, the following can be highlighted: (1) an increase in grain size through the
286 unconformity, marked by the abrupt occurrence of sandy conglomerate deposits over
287 medium to coarse-grained sandstones; (2) the presence of sandstone clasts and
288 reworked fossil trunks of the Sequence II in basal conglomerate of sequence III; (3) a
289 change in the direction of the fluvial palaeocurrents through the unconformity (Figure
290 2). The top of Sequence III is also marked by disconformity, marked by onlap of the

291 fluvial and deltaic deposits of Sequence IV (Abaiara Formation) (Figures 2 and 6).
292 Sequence III is composed of two distinct facies association (Figure 7): (1) Fluvial
293 Sheetflood Facies Association and (2) *Braided Fluvial Channel Belt Facies Association*.

294

295 3.3.1 Fluvial Sheetflood Facies Association

296

297 This facies association is composed of sandy conglomerate and medium to very
298 coarse-grained sandstones, moderately sorted, arranged in sheet-like sandstone
299 bodies, 0.5 and 1.2 m thick. The conglomerates are clast-supported, massive and
300 predominantly consist of granules and pebbles of quartz, granites, sandstones and
301 muddy intraclasts (Gm). The sandstones, in turn, are massive (Sm) or, less often,
302 display low-angle cross-stratifications (SI). The sandstones commonly display granules
303 or pebbles of granite or mud intraclasts, dispersed or concentrated along the
304 stratification planes.

305 The dominance of massive conglomerates together with massive or horizontal
306 to low-angle stratified sandstones, displayed in sedimentary bodies with sheet
307 geometry, suggests that these deposits result from high-energy, sheetflood fluvial flows
308 (Nemec and Postma, 1993; Blair, 2000, 2001). The succession of amalgamated
309 sandstone and conglomerate beds may represent a series of flooding events that were
310 deposited in wide shallow channels. Massive, clast supported conglomerate suggests
311 deposition by high-density hyperconcentrated flows. Massive sandstone is interpreted
312 as rapid deposition from heavily sediment-laden flow during waning floods
313 hyperconcentrated flows. Low-angle cross-stratified sandstones are interpreted as
314 plane bedforms produced near the upper to lower flow regime transition by
315 unidirectional currents (Miall, 1996).

316

317 3.3.2 Braided Fluvial Channel Belt Facies Association

318

319 This facies association is made up of several sheet-like sandstone bodies, 2 to
320 7 m thick, bounded at the base by flat to concave-up erosional surfaces, sometimes
321 marked by massive, granule to pebbled clast-supported conglomerate (Gcm), 10 to 20
322 cm thick. These deposits are succeeded by 0.2 to 0.4 m thick, trough (St) and planar
323 (Sp) cross-stratified sandstones, and, rarely, by low-angle cross-stratified sandstones
324 (SI) (Figure 7). Sometimes, it can be observed compound cross-strata, 2 and 4 m thick,
325 in which each set is bounded by inclined surfaces (5-8°) that dip in the same direction
326 of the cross-strata. Measurements of the direction of the dip of the cross-strata indicate
327 a paleocurrent toward the SW to NW (Figure 2).

328 These sandstone bodies are interpreted as deposits of fluvial channel, based on
329 the presence of concave-up erosional lower boundaries and dominance of
330 unidirectionally oriented decimetre-scale planar and trough cross-strata. The erosional
331 lower boundary of the sandstone bodies may be interpreted as limits of the fluvial
332 channels, equivalent to the 5th-order surface of Miall (1988, 1996). The downcurrent-
333 dipping inclined strata represent downstream accretion of compound bars with
334 superimposed, small-scale bedforms (DA architectural element of Miall, 1988, 1996).
335 The sheet geometry of the sandstone bodies, dominantly coarse sand size of the
336 deposits, absence of mudstone, locally developed downstream accretion macroforms
337 and low dispersion of the paleocurrent data collectively suggests that this facies
338 association represents braided fluvial channel belt deposits (Miall, 1996; Ray and
339 Chakraborty, 2002).

340

341 **3.4 Sequence IV**

342 Sequence IV is approximately 400 m thick and corresponds lithostratigraphically
343 to the Abaiara Formation (Figure 2). It is bounded at the base by an unconformity
344 marked by onlap of deltaic deposits over fluvial braided channel belt facies association
345 of Sequence III (upper section of the Missão Velha Formation) (Figure 7). The upper
346 contact of this sequence is marked by angular unconformity with the alluvial strata of
347 the Barbalha Formation (Assine, 1990) or the Rio da Batateira Formation (Ponte,
348 1990), which compose the base of the Post-Rift Supersequence (Assine, 2007).
349 Sequence IV is composed of four distinct facies association (Figures 2, 7 and 8): (1)
350 the Prodelta/Deltaic Front, (2) Distributary Fluvial Channels, (3) Overbank Deposits and
351 (4) Meandering Fluvial Channel Facies Association.

352

353 3.4.1 Prodelta / Delta Front Facies Association

354

355 This facies association is characterized by repetition of 2 to 10 m meter-scale
356 coarsening-upward cycles (Figure 8). The base of the cycles is characterised by
357 reddish to greenish color, massive (Fm) or laminated (Fl) mudstones, frequently
358 exhibiting ostracod fossils. These mudstones interlayer upward with fine to very fine
359 sandstones, 5 and 30 cm thick, which exhibit ripple cross-laminations (Sr) and, less
360 commonly, low-angle cross stratifications (Sl). The transition between mudstones and
361 sandstones beds is marked by soft-sediment deformations structures, including simple
362 load, pendulous features, pseudo-nodules and balls and pillow structures. Some
363 cycles can present at the top amalgamated layers of fine to medium sandstones with

364 trough (St) and planar (Sp) cross-stratifications. The sandstones may also show
365 indication of soft-sediment deformation, mainly oversteepened cross-stratification,
366 convoluted folds and plate and pillar structures. Measurements of the direction of the
367 dip of the cross-strata show a preferential direction within each cycles, though with high
368 dispersion if different cycles are compared (Figures 2 and 8).

369 The lithology, coarsening-upward cycles organization and dominance of
370 unidirectional current-generated structures suggest that these facies association
371 represents progradation of river-dominated delta, similar to those described by
372 Bhattacharya (1991) and Giosan and Battacharya (2005). The ostracod fossils present
373 in the fine-grained deposits indicate a lacustrine context (Coimbra et al., 2002). The
374 thickness of the cycles represents the minimum depth of the water level, which, in this
375 case, varied from 2 to 10 m. The massive and laminated mudstones at the base of the
376 cycles are interpreted as prodelta deposits. The lack of bioturbation in these deposits
377 indicates that the sediment was rapidly buried, thus preventing the reworking of the
378 substrate by organisms. The vertical increase in the frequency and thickness of the
379 sandstones layers indicate progradational tendency of the deltaic front. The
380 pronounced intercalation of sandstones and mudstones and the dominance of the
381 unidirectional current-generated structures in the sandstones suggest that the
382 sediments were supplied by intermittent unidirectional flows derived from fluvial
383 systems. The presence of different types of soft-sediment deformation in the contacts
384 between the sandstones and mudstones and within the sandstones layers must be
385 linked to a high rate of sedimentation, which increases the water pressure in the pores,
386 inducing the liquification of the sediment. The amalgamated sandstones that occur at
387 the top of the coarsening-upward cycles must represent the proximal portions to the
388 delta front, deposited by distributary mouth-bars (Battacharya, 2011).

389

390 3.4.2 Distributary Fluvial Channel Facies Association

391

392 This facies association is made up by fining-upward successions, 1.5 to 5 m
393 thick, normally overlaying Prodelta / Deltaic Front Facies association (Figure 8). The
394 base of the cycles is marked by an erosive surface, frequently capped by
395 intraformational conglomerates rich in mudstone intraclasts. Internally, the cycles are
396 characterised at the base by medium to coarse-grained sandstones, moderately
397 sorted, with trough cross-stratifications (St), planar cross-stratifications (Sp) and low-
398 angle cross-stratifications (Sl), which sometimes give rise toward the top to fine to very
399 fine-grained sandstones with ripples cross-laminations (Sr).

400 The presence of fining upward cycles, bound by erosive surfaces capped by
401 intraclast lags suggests deposits of fluvial channels. The fact that this association
402 invariably covers prodelta/ deltaic front deposits indicates distributary fluvial channels
403 of the deltaic plain (Hampson et al., 1999). The trough and planar cross-stratifications
404 sandstones may be interpreted as deposits of 2D and 3D subaqueous dunes,
405 respectively, which migrate over the bottom of the channel in response to unidirectional
406 tractional flows. The fining-upward successions suggest a progressive decrease of the
407 flow velocity, culminating in the abandonment of the channel. The lack of lateral
408 accretion surfaces suggests fluvial channels with low sinuosity.

409

410 3.4.3 Overbank Facies Association

411 This facies association commonly occurs intercalated with distributary fluvial
412 channel or meandering fluvial channels deposits. It is characterised by red or greenish
413 (rare) mudstones occasionally interlayered with tabular sandstones, where deposits
414 commonly exhibit a tabular geometry, ranging from 3 to 15 m thick (Figure 8). The
415 mudstones are massive (Fm) or laminated (Fl), sometimes displaying calcareous
416 concretions. The nodules vary from 1 to 20 cm in diameter, exhibiting shapes that
417 range from highly irregular to vertically elongated and tabular. The sandstones are fine
418 to medium-grained, well-sorted, arranged in tabular layers, with planar and non-erosive
419 basal contact, internally compound by ripples cross-laminations (Sr). Sometimes, very
420 fine to coarse-grained, bimodal sandstones, with low-angle cross-stratifications (Sl(e)),
421 can be observed. Each lamina is inversely graded, 1 and 3 mm thick.

422 This facies association is interpreted as overbank deposits, which may have
423 been accumulated both in the inter-distributary bays present in the deltaic plain or in
424 the swampy regions of the fluvial floodplain. The mudstones have been deposited due
425 to the gravitational settling of particles in suspension, while the sandstones with ripples
426 cross-laminations represent the deposits of crevasse splays accumulated during river
427 channel overbank flooding. The carbonate nodules horizons are interpreted as
428 calcareous palaeosols (Ray and Chakraborty, 2002). The sandstones with low-angle
429 cross-stratification, with inversely gradated laminae, are interpreted as aeolian sand
430 sheet deposits formed by the migration and climbing of the aeolian ripples (Scherer &
431 Lavina, 2005; Scherer et al., 2007). The presence of frequent carbonaceous
432 palaeosols and aeolian deposits, indicates drier periods marked by a water table falling
433 and subaerial exposure of the depositional surface.

434

435 3.4.4 Meandering Fluvial Channel Facies Association

436

437 This facies association is composed of sandstone bodies, 2 to 7 m thick,
438 bounded at the base by erosive, concave upward surfaces, with reliefs varying from 1
439 to 3 m. Internally each sandstone body shows one large scale lateral accretion unit,
440 characterized by sets of fine to medium-grained sandstones with trough cross-
441 stratification (St) and/or ripples cross-lamination which are bounded by inclined
442 surfaces (2 to 10°) that dip approximately perpendicular to the direction of the cross-
443 strata dip (Figure 9)

444 The presence of sandbodies with an erosive base and the predominance of
445 unidirectional tractive structures allow to interpret this facies association as fluvial
446 channel deposits. The occurrence of large-sized inclined strata indicates the presence
447 of macroforms filling the fluvial channels. The fact that the cross-strata show
448 palaeocurrents that are approximately transversal to the direction of the dip of the
449 bounding surfaces suggests lateral accretion macroforms (Miall, 1996). The dominance
450 of lateral accretion macroform suggests that this facies association represents high
451 sinuosity fluvial channel (Ghazi and Mountney, 2010).

452

453 3. Stratigraphic evolution

454

455 The Neo-Jurassic-Neocomian succession of the Araripe Basin consists of four
456 depositional sequences bound by unconformities (Figure 2). Sequence I corresponds
457 lithostratigraphically to the Brejo Santo Formation and can be interpreted as the distal
458 portion of an aluvial plain that developed in an arid to semi-arid climatic context. This
459 sequence is composed of floodplain and fluvial sheetflood facies associations that flow
460 toward the SSE (Figure 2 e Figure 11a). This depositional context suggests that the
461 basin extends toward the north, where the proximal sub-environments of Sequence I
462 would be positioned. Therefore, the entire depositional system can represent a
463 distributary fluvial or terminal fans systems that occupied an area much larger than the
464 one circumscribed within the current erosive limits of the Araripe Basin, as claimed by
465 Kuchle et al. (2011).

466 Sequence II, corresponding to the lower portion of the Missão Velha Formation,
467 is characterized by multi-storey and multi-lateral, amalgamated, sheet sandstone
468 bodies with rare preservation of fine-grained, overbank deposits, interpreted as the
469 deposits of braided fluvial channel-belt system, with palaeocurrents toward the SE
470 (Figure 2 e Figure 11b). The disconformity that separates Sequences I and II is easily
471 observed in outcrops, marked by grain-size increase and by abrupt change in
472 depositional style, from an ephemeral fluvial system of Sequence I to a braided fluvial

473 channel-belt system of Sequence II. The change in the depositional style reflects
474 change in the discharge regime of the fluvial systems, which is probably associated
475 with the more humid climatic conditions in Sequence II. Although there is a change in
476 the depositional systems of sequences I and II, both units have palaeocurrent to SE.
477 This suggests that the source area and proximal deposits of the sequences I and II
478 were northwest of the study area.

479 Sequence III, corresponding to the upper interval of the Missão Velha
480 Formation, is composed, at its base, of fluvial sheetflood facies association that passes
481 upward to braided fluvial channel belt facies association, the latter displaying facies
482 architecture similar to that of the fluvial deposits of Sequence II, though with
483 characteristically distinct palaeocurrents (Figure 11c). The fluvial strata of Sequence II
484 exhibit palaeocurrents toward the SE, while the fluvial deposits of Sequence III display
485 a palaeocurrent pattern predominantly toward the SW and NW (Figure 2). So, the
486 unconformity between Sequences II and III marks significant rearrangement in the
487 depocenters of the basin. The presence of sandstones clasts and reworked coniferous
488 trunks of the sequence II at the base of the Sequence III indicates uplift of the basin,
489 exposing the sequence II deposits to erosion. This fact, combined with the change in
490 the fluvial palaeocurrent vectors, must be associated with tectonic movements that
491 changed the morphology of the basin, causing a change in the drainage system.

492 Sequence IV, equivalent to the Abaiara Formation, is characterised by a thick
493 succession deposited by deltaic and fluvial systems, that display high dispersion in the
494 palaeocurrents (Figure 2 and 10), suggesting that the sedimentation occurred within a
495 restricted basin with sedimentary supply from different flanks of the basin (Figure 11d).
496 The onlap of the deltaic deposits of Sequence IV over the fluvial sandstones of
497 Sequence III (Figure 7) confirms the restructuring of the basin with consequent
498 reduction of the depositional area.

499 **4. Tectonic-Stratigraphic Context**

500 In recent years, different studies have discussed the tectonic-stratigraphic
501 evolution of rift basins, identifying different evolutionary stages (Morley, 2002). The first
502 stage is characterised by incipient extensional efforts that generate a basin that has a
503 broadly synclinal geometry. The thickening toward the basin center is achieved by
504 expansion of section across numerous rotational and nonrotational normal faults.
505 These faults are of similar displacement and no dominant fault trend is apparent. This
506 large basin was established before the development of the half graben system. Thus,
507 this stage is characterized by a wide synclinal depression, larger than the subsequent

508 rift trough, associated to the low rate, continuous and uniformly distributed tectonic
509 activity (Morley, 2002; Kinabo et al., 2007; Kuchle et al., 2011). Although different
510 authors (e.g., Prosser, 1993; Bosence, 1998; Gawthorpe and Leeder, 2000) visualise
511 the beginning of the rift in the form of smaller-sized half graben basins bounded by
512 small normal faults, some actual and ancient examples corroborate the synformal basin
513 geometry to early rift stage (Morley, 2002; Kinabo et al., 2007; Kuchle et al., 2011). In
514 turn, the second stage would be marked by the formation of half-grabens. The
515 development of half-grabens would occur through the nucleation of the main border
516 fault by linkage of smaller faults. In the initial phase of the process, the mechanical
517 subsidence is still reduced, as a result of the small slip faults (Gawthorpe and Leeder,
518 2000). Accordingly, the fault scarps are underdeveloped, reducing the occurrence of
519 conglomerate wedges (Prosser, 1993; Bosence, 1998; Gawthorpe and Leeder, 2000).
520 When the fault linkage occurs, forming a continuous border fault along the half-graben,
521 there is an increase in the subsidence favouring the development of large and deep
522 lakes, as now occurs in the rift system of East Africa. As the rate of accommodation
523 creation tends to be greater than the rate of sedimentary influx, the sedimentary
524 succession displays retrogradational stacking pattern (Prosser, 1993; Kuchle and
525 Scherer, 2010). Finally, there is the final filling stage of the half-graben, in which the
526 movement of the border fault is significantly reduced. Therefore, there is a decrease in
527 the ratio between the rate of accommodation creation and the rate of sedimentary
528 influx, resulting in a progradational stacking pattern (Prosser, 1993; Kuchle and
529 Scherer, 2010).

530 The Jurassic-Neocomian section of the Araripe Basin exhibits distinct
531 stratigraphic signatures, which allow for the identification of different evolutionary
532 stages. Sequences I, II e III, equivalent to Brejo Santo and Missão Velha formation,
533 show depositional systems distribution and palaeocurrent pattern indicating that this
534 units occupied a depositional area much larger than the one circumscribed within the
535 current erosive limits of the Araripe Basin. This suggests that sequences I, II and III
536 were deposited in a large sedimentary basin connected to the initial stage of the
537 Neocomian rifting (Kuchle et al., 2011). Previous studies (e.g. Estrela, 1972; Garcia et
538 al., 2005; Kuchle et al., 2011) have suggested that Brejo Santo and Missão Velha
539 formations were accumulated on the northern flank of the one large endorheic basin,
540 named of Afro-Brasilian Depression. However, the difference of the fluvial
541 palaeocurrent between sequences II and III marks a regional rearrangement of the
542 drainage system possibly related to tectonic activity. These tectonic movements may
543 have compartmentalised the large endorheic basin, defining more localised drainage

544 basins separated by internal highs, as observed in other basins of the Brazilian
545 Northeast (Kuchle et al., 2011).

546 Because the deposits of Sequences I, II and III are linked to the initial rifting
547 stages, it is inadvisable to use the term pre-rift to designate the tectonic stage in which
548 this entire sedimentary section is inserted, as has been employed in previous studies
549 (Ponte and Appi, 1990; Assine, 1990,1992; Ponte, 1992; Assine, 1994; Ponte and
550 Ponte Filho, 1996; Assine, 2007). The term pre-rift is used to designate rocks that are
551 completely unrelated to the rifting process, consisting of the sedimentary basement
552 upon which the taphrogenic processes will act (Prosser, 1993; Bosence, 1998).
553 Normally, the pre-rift strata are tens to hundreds of millions of years older than the
554 deposits accumulated during the rifting event (Bosence, 1998). The most appropriate
555 term for this initial phase of accumulation would be the Early Rift Stage (Morley, 2002)
556 or the Initial Rift Tectonic Systems Tract (Kuchle and Scherer, 2010). Sequence IV, in
557 turn, is characterised by a thick succession of fluvial-deltaic-lacustrine deposits,
558 indicative of a context with a high rate of accommodation generation. Beside, the high
559 variation in the palaeocurrent direction and the fact that Sequence IV strata onlap
560 deposits from Sequence III are consistent with the implantation of half-grabens
561 (Bosence, 1988; Prosser, 1993; Galthorpe and Leeder, 2000). According Prosser
562 (1993) the sedimentary influx of the half-grabens occurs from different regions (e.g.,
563 flexural margin, faulted margin and axial influx), resulting in a high dispersion of
564 palaeocurrents trends when different sectors or stratigraphic intervals in the basin are
565 analyzed, similar to what can be observed in the deposits of Sequence IV. The
566 presence in outcrops of growth faults affecting deposits of Sequence IV corroborates
567 the idea of intense extensional tectonics concomitant with sedimentation (Aquino,
568 2009). Thus, Sequence IV may be considered the record of the Half-Graben Stage
569 (Morley, 2002) or of the Half Graben Develop to Rift Climax Tectonic SystemsTracts
570 (Kuchle and Scherer, 2010).

571

572 **5. Conclusions**

573

574 It was possible to individualise four depositional sequences in the Jurassic-
575 Neocomian section of the Araripe Basin. Sequence I, equivalent to the Brejo Santo
576 Formation, is composed of deposits from sheet floods and of floodplains. Sequences II,
577 correspondent to the lower portion of Missão Velha Formation, is characterised by
578 braided fluvial channels belt amalgamated sandbodies intercalated with rare and
579 discontinuous floodplain deposits. Sequence III, correspondent to the upper portion of
580 Missão Velha Formation, is composed of fluvial sheetflood deposits, which are overlain

581 by braided fluvial channel belt deposits. Sequence IV, equivalent to the Abaiara
582 Formation, is composed of fluvial-deltaic-lacustrine deposits.

583 The sequences were accumulated during different rift tectonic stages. Sequences I
584 and II were deposited over a large basin, similar to a syncline, though linked to the
585 initial stages of rifting. The change in the direction of the palaeocurrents of Sequence III
586 (toward the SW or NW) in relation to that of the palaeocurrents of Sequences I and II
587 (toward the SSE) is associated with tectonic movements related to the beginning of the
588 implantation of internal highs and grabens in an important structural reorganisation of
589 the basin. Sequence IV, in turn, was accumulated in well-defined half-graben systems
590 with the development of lacustrine environment, including fluvial and deltaic systems.
591 The sedimentary influx of the half-grabens occurs from different regions (e.g., flexural
592 margin, faulted margin and axial influx), as attested by high dispersion of
593 palaeocurrents trends of the Sequence IV.

594 From the results of this work it is possible to visualize the evolution of the different
595 stratigraphic stages of rifting. Corroborating propositions of Morley (2002), Kinabo et al.
596 (2007) and Kuchle et al. (2011), the first stage of rifting (sequences I and II) is
597 characterized by the development of a wide basin, unlike the model of Prosser (1993),
598 Bosence (1998), Gawthorpe and Leeder (2000) that suggest the existence of small
599 grabens isolated at the beginning of rifting. This large basin has a relatively low rate of
600 subsidence (low A / S ratio), and does not record extensive lacustrine facies. The
601 development of half-graben system occurs at a later stage. Firstly, there is the
602 subdivision of large basin into incipient graben (Sequence III), even with low rate of
603 subsidence. After, from the linkage of fault segments occurs an increase in the
604 subsidence (increase in A/S ratio) and full development of half graben systems,
605 allowing the development of deep and extensive lakes (Sequence IV).

606

607 **Acknowledgements:**

608 The authors acknowledges PETROBRAS for financing the research project. CMSS
609 acknowledge the Brazilian Research Council (CNPq) for research support. We are also
610 grateful for the constructive and thoughtful reviews by Reinhardt Fuck, Giorgio Basilici,
611 Michael Holz and an anonymous referee.

612

613 **References:**

614

615 Allen, J.R.L. and Leeder, M.R., 1980. Criteria for instability of upperstage plane beds.
616 *Sedimentology* , 27, 209–212.

617

- 618 Aquino, M.M., 2009. A Formação Abaiara e o Arcabouço Tectonoestratigráfico da
619 Região de Abaiara-Brejo Santo, Bacia do Araripe, NE do Brasil. MSc. thesis, Centro de
620 Ciências Exatas e da Terra, Universidade Federal do Rio Grande do Norte.
621
- 622 Assine, M.L., 1990. Sedimentação e tectônica da Bacia do Araripe (Nordeste do
623 Brasil). MSc. thesis, Universidade Estadual Paulista.
624
- 625 Assine, M. L., 1992. Análise estratigráfica da bacia do Araripe, Nordeste do Brasil.
626 Revista Brasileira de Geociências, 22(3), 289-300.
627
- 628 Assine, M.L. 1994. Paleocorrentes e paleogeografia na Bacia do Araripe, Nordeste do
629 Brasil. Revista Brasileira de Geociências, 24 (4), 1-10.
- 630 Assine, M.L. 2007. Bacia do Araripe. Boletim de Geociências da Petrobras, 15 (2),
631 371-389.
632
- 633 Bhattacharya, J. P. 1991. Regional to subregional facies architecture of river-
634 dominated deltas in the Alberta sub-surface, Upper Cretaceous Dunvegan Fm. In:
635 Miall, A.D and Tyler (Eds.), The 3-D facies architecture of terrigenous clastic sediments
636 and its implications for hydrocarbon discovery and recovery. SEPM Concepts in
637 Sedimentology and Paleontology 3, 189-206.
638
- 639 Bhattacharya, J.P. 2011. Deltas. In: James, N.P. and Dalrymple, R.W. (Eds), Facies
640 Model 4. Geological Society of Canada, 233-264.
641
- 642 Blair, T.C. 2000. Sedimentology and progressive tectonic unconformities of the
643 sheetflood-dominated Hell.s Gate alluvial fan, Death Valley, California. Sedimentary
644 Geology, 132, 233-262.
645
- 646 Blair, T.C. 2001. Outburst flood sedimentation on the proglacial Tuttle Canyon alluvial
647 fan, Owens Valley, California, U.S.A. J. Sediment. Res., 71, 657-679.
648
- 649 Bosence, D.W.J., 1998. Stratigraphic and sedimentological models of rift basins. In:
650 Purser, B.H., Bosence, D.W.J. (Eds.), Sedimentation and Tectonics of Rift Basins: Red
651 Sea - Gulf of Aden. Chapman & Hall, London, 9-25.

652

653 Cardoso, F. M. C. 2010. O grabén da Palestina: contribuição à estratigrafia e estrutura
654 do estágio rifte na Bacia do Araripe, Nordeste do Brasil. MSc. thesis, Centro de
655 Ciências Exatas e da Terra, Universidade Federal do Rio Grande do Norte.

656

657 Cardoso, F. M. C., Jardim de Sá, E. F., Silva, F. C. A., Scherer . C. M. S. 2009. O
658 Graben do Serrote das Cacimbas-Palestina (Sub-bacia Cariri, Bacia do Araripe, NE,
659 Brasil). In: XXIII Simpósio de Geologia do Nordeste, Fortaleza, Resumos.

660

661 Cardoso, F.M.C., Jardim de Sá, E.F., Scherer, C.M.S., Córdoba, V.C., Antunes, A.F.,
662 Silva, F.C.A., 2010. Tectono-stratigraphic relationships in the Palestina Graben,
663 Araripe Basin, NE Brazil. II Central and North Atlantic Conjugate Margins Conference,
664 Lisboa, Abstracts, v. 1.

665

666 Catuneanu, O., 2006. Principles of Sequence Stratigraphy. Elsevier, Amsterdam, 375
667 pp.

668

669 Chakraborty, T., 1999. Reconstruction of fluvial bars from the Proterozoic Mancherai
670 Quartzite, Pranhita-Godavari, India. In: Smith, N.D., Rogers, J.(Eds.), Fluvial
671 Sedimentology IV, IAS Spec. Pub., 28, 451–466.

672

673 Chang, H.K., Kowsmann, R.O., Figueiredo, A.M.F., Bender, A.A., 1992. Tectonics and
674 stratigraphy of the East Brazil Rift System: an overview. Tectonophysics, 213, 97-138.

675

676 Costa, A B.S., 2012. Diagênese e Proveniência dos Arenitos da Tectonossequência
677 Rifte nas bacias do Rio do Peixe e do Araripe, NE do Brasil. MSc. thesis, Centro de
678 Ciências Exatas e da Terra, Universidade Federal do Rio Grande do Norte.

679

680 Coimbra, J.C., Arai, M., Carreno, A.L., 2002. Biostratigraphy of Lower Cretaceous
681 microfossils from the Araripe basin, northeastern Brazil. Geobios, 35 (6), 687-698.

682

683 Córdoba, V.C., Jardim de Sá, E.F., Sousa, D.C., Antunes, A.F., Cruz, L.R., 2008. Bacia
684 Pernambuco-Paraíba. Boletim de Geociências da PETROBRAS, 15, 391-403.

685

686 Estrella, G.O., 1972. O estágio rift nas bacias marginais do leste brasileiro.

687 26 Congresso Brasileiro de Geologia, Belem,. Anais, v. 3, p. 29-34.

688

- 689 Fambrini, G.L., Lemos, D.R., Tesser, S., Araújo, J.T., Silva Filho, W.F., Souza, B.Y.C.,
690 Neumann, V.H.M.L. 2011. Estratigrafia, arquitetura deposicional e faciologia da
691 Formação Missão Velha (Neojurássico-Eocretáceo) na área-tipo, Bacia do Araripe,
692 Nordeste do Brasil: exemplo de sedimentação de estágio de início de rifte a clímax de
693 rifte. *Revista do Instituto de Geociências – USP*, 11 (2), 55-8.
694
- 695 Françolin, J. B. L., Cobbold, P.R., Szatmari, P., 1994. Faulting in the Early Cretaceous
696 Rio do Peixe Basin (NE Brazil) and its significance for the opening of the Atlantic.
697 *Journal of Structural Geology*, Amsterdam, 16 (5), 647-661.
698
- 699 Gawthorpe, R.I., Leeder, M.R., 2000. Tectono-sedimentary evolution of active
700 extensional basins. *Basin Research*, 12 (2), 195-218.
701
- 702 Garcia, A.J.V., Rosa, A.A.S., Goldberg, K., 2005. Paleoenvironmental and
703 paleoclimatic control on early diagenetic processes and fossil record in Cretaceous
704 continental sandstones of Brazil. *Journal of South American Earth Sciences*, 19,
705 243-258.
706
- 707 Garcia, H. R. C. 2009. Arquitetura deposicional e evolução tectonoestratigráfica das
708 seqüências Pré-Rifte e Rifte, na porção central do Vale do Cariri, Bacia do Araripe, NE
709 do Brasil. MSc. thesis, Centro de Ciências Exatas e da Terra, Universidade Federal do
710 Rio Grande do Norte.
711
- 712 Ghazi, S., Mountney, N.P., 2010. Facies and architectural element analysis of a
713 meandering fluvial succession: The Permian Warchha Sandstone, Salt Range,
714 Pakistan. *Sedimentary Geology*, 221, 99–126.
715
- 716 Giosan, L., Bhattacharya, J.P. 2005. River deltas: Concepts, models and examples.
717 *SEPM Special Publications*, 83.
718
- 719 Guignone, J.I., Couto, E.A., Assine, M.L., 1986. Estratigrafia e estrutura das bacias do
720 Araripe, Iguatu e Rio do Peixe. *Anais do Congresso Brasileiro de Geologia*, 34, 271-
721 285.
722
- 723 Hampton, B.A., Horton, B.K., 2007. Sheetflow fluvial processes in a rapidly subsiding
724 basin, Altiplano plateau, Bolivia. *Sedimentology*, 1-27
725

- 726 Kinabo, B.D., Atekwana, E.A., Hogan, J.P., Modisi, M.P., Wheaton, D.D., Kampunzu,
727 A.B. 2007. Early structural development of the Okavango rift zone, NW Botswana.

728 Journal of African Earth Sciences, 48, 125-136.
- 729
730 Kuchle, J., Scherer, C.M.S., Born, C.C., Alvarenga, R.S., Adegas, F. 2011. A
731 contribution to regional stratigraphic correlations of the Afro-Brazilian depression e The
732 Dom João Stage (Brotas Group and equivalent units e Late Jurassic) in Northeastern
733 Brazilian sedimentary basins. Journal of South American Earth Sciences, 31, 358-371.
734
735 Kuchle, J.; Scherer, C.M.S. 2010. Sismoestratigrafia de bacias rifte: técnicas, métodos
736 e sua aplicação na Bacia do Recôncavo. Boletim de Geociências da Petrobras, 18(2),
737 33-60.
738
739 Jardim de Sá, E.F., Antunes, A.F., Cordoba, V.C., Vasconcelos, P.M.P, Scherer,
740 C.M.S, Silva, F.C.A., Souza, D.C., Cruz, L.R., Nascimento, M.A., Almeida, C.B.,
741 Aquino, M.M., Cardoso, F.C., Medeiros, W.E., Lins, F.A.P.L., 2011. Structural,
742 Stratigraphy and Geochronological Constraints of the Mesozoic Rifting in Northeast
743 Brazil, Bearing to the Opening of the South Atlantic. Gondwana 14, Búzios, v.1, p.224.
744
745 Jardim de Sá, E.F., Antunes, A.F., Cordoba, V.C., Alvez da Silva, F.C., Souza, D.C.,
746 Cruz, L.R., Almeida, C.B., Medeiros, W.E. 2010. Evolução do rifte na Margem Leste-
747 Setentrional Brasileira: contribuição dos projetos ANP/UFRN/PPGG. 45 Congresso
748 Brasileiro de Geologia, Belém, Resumos, p.224.
749
750 Jardim de Sá, E.F., Sousa, D.C., Aquino, M.M., Scherer, C.M.S.; Córdoba, V.C., 2009.
751 A Tectonossequencia Rifte na Bacia do Araripe. XXIII Simpósio de Geologia do
752 Nordeste, Fortaleza, Resumos, p.152.
753
754 Jo, H.R., Chough, S.K., 2001. Architectural analysis of fluvial sequences in the
755 northwestern part of Kyongsang Basin (Early Cretaceous), SE Korea. Sedimentary
756 Geology, 144, 307-334.
757
758 Matos, R.M.D., 1992. The Northeast Brazilian rift system. Tectonics, 11, 766-791.

759

760 Matos, R.M.D., 1999. History of the Northeast Brazilian rift system: kinematic
761 implications for the break-up between Brazil and West Africa. In: Cameron, N.R., Bate,
762 R.H., Clure, V.S. (Eds.), The oil and gas habitats of the South Atlantic. Special
763 Publications of Geological Society of London, 55-73.

764

765 Miall, A.D., 1977. A review of the braided river depositional environment. *Earth-Sci.*
766 *Rev.* 13, 1-62.

767 Miall, A.D., 1996. *The Geology of Fluvial Deposits: Sedimentary Facies, Basin Analysis*
768 *and Petroleum Geology*. Springer-Verlag, New York.

769

770 Miall, A.D., 1988. Facies Architecture in clastic sedimentary basins. In: Kleinspehn,
771 K.L. and Paola, C. (Eds.), *New perspectives in basin analysis*. Springer-Verlag, Berlin,
772 67–81.

773

774 Miall, A.D., Arush, M., 2001. Cryptic sequence boundaries in braided fluvial
775 successions. *Sedimentology*, 46, 971-985.

776

777 Mitchum, R.M., Vail, P.R., Thompson III, S., 1977. Seismic stratigraphy and global
778 changes of sea level. Part 2: the depositional sequence as a basic unit for stratigraphic
779 analysis. In: Payton, C.E. (Ed.), *Seismic Stratigraphy — Application to Hydrocarbon*
780 *Exploration*. Am. Assoc. Pet. Geol. Mem., 26, 53–62.

781

782 Morley, C.K., 2002. Evolution of large normal faults: Evidence from seismic reflection

783 data. *American Association of Petroleum Geologists Bulletin*, 86, 961-978.

784

785 Nemeček, W., Postma, G., 1993. Quaternary alluvial fans in southwestern Crete:
786 sedimentation processes and geomorphic evolution. In: Marzo, M., Puigdefabregas, C.
787 (Eds.), *Alluvial sedimentation*. IAS Spec.Pub., 17, 235-276.

788

789 Ponte, F.C. and Ponte Filho, F.C. 1996. *Estrutura geológica e evolução tectônica da*
790 *Bacia do Araripe*. DNPM, Recife, 68pp.

791

- 792 Ponte, F.C. and Appi, C.J. 1990. Proposta de revisão da coluna litoestratigráfica da
793 Bacia do Araripe. 36 Congresso Brasileiro de Geologia, Natal, Anais, v.1, p.211-226.
794
- 795 Prosser, S., 1993, Rift-related linked depositional systems and their seismic
796 expression. In: Williams, G.D., Dobb, A. (Eds), Tectonics and seismic sequence
797 stratigraphy. Geological Society Special Publication 71,117–144.
798
- 799 Ray, S.; Chakraborty, T., 2002. Lower Gondwana fluvial succession of the Pench–
800 Kanhan valley, India: stratigraphic architecture and depositional controls. *Sedimentary
801 Geology*, 151, 243-271.
802
- 803 Scherer, C.M.S.; Lavina, L.E.C.; Dias Filho, D.C.; Oliveira, F.M.; Bongiolo, D.E.; Silva,
804 E., 2007. Stratigraphy and fácies architecture of the fluvial-aeolian-lacustrine Sergi
805 Formation (Upper Jurassic), Recôncavo Basin, Brazil. *Sedimentary Geology*, 194, 169-
806 193.
807
- 808 Scherer, C.M.S. and Lavina, E.L.C., 2005. Sedimentary cycles and facies architecture
809 of aeolian–fluvial strata of the Upper Jurassic Guar Formation, Southern Brazil.
810 *Sedimentology* 52, 1323–1341.
811
- 812 Smith, N.D., Cross, T.A., Dufficy, J.P., Clough, S.R., 1989. Anatomy of an avulsion.
813 *Sedimentology*, 36, 1–23.
814
- 815 Spalletti, L.A., Piol, F.F., 2005. From Alluvial Fan to Playa: An Upper Jurassic
816 Ephemeral Fluvial System, Neuqun Basin, Argentina. *Gondwana Research*, 8, 362-
817 382.
818
- 819 Tucker, M.E., 1996. *Sedimentary Rocks in the Field*. John Wiley and Sons,
820 Chinchester, England.
821
- 822 Tunbridge, I.B., 1984. Facies models for a sandy ephemeral stream and clay playa
823 complex; the Middle Devonian Trentishoe Formation of North Devon, UK.
824 *Sedimentology*, 31, 697–716.
825
826
827

828

829

830

831

832

833

834

835

836

837

838

839 **Figure Captions**

840 Table 1: Stratigraphic nomenclature table of the Araripe Basin (according Assine,
841 2007)

842

843 Table 2: Summary of facies description and interpretation.

844

845 Figure 1: (A) Regional geological setting of the Araripe Basin. (B) Simplified geological
846 map of the studied area showing the location of eight logged sections, which represent
847 the study localities discussed in this paper.

848

849 Figure 2: (A) Stratigraphic cross-section based on log correlation, displaying the
850 depositional sequences, their bounding surfaces and facies association (datum:
851 regional flooding surface at the base of the Abaiara Formation). (B) Explanation of
852 symbols used in the sedimentological logs of this paper.

853

854 Figure 3: (A) Sedimentological log showing litofacies, facies association and facies
855 succession of the Sequence I. See Figure 2 for explanation of symbols and position of
856 the logs. See Table 1 for facies code. (B) Lithofacies Sr. Ripple cross-laminated, fine-
857 grained sandstone. Pencil: 0.15m. (C) Lithofacies Fm. Massive mudstone. Coin:
858 20mm.

859

860 Figure 4: (A) Sedimentological log showing the basal and the top unconformities of the
861 Sequence II. See Figure 2 for explanation of symbols and position of the logs. See
862 Table 1 for facies code. (B) Low relief, basal unconformitie marked by abrupt contact
863 between floodplain (Sequence I) and braided fluvial channel (Sequence II) facies
864 associations. Person: 1.7 m. (C) Sandy conglomerate with sandstones clasts

865 (Lithofacies Gm) of the Sequence III covering braided fluvial channel sandstones of
866 Sequence II. Observe erosive nature of the contact. Hummer: 0.3 m.

867

868 Figure 5: (A) Sedimentological log showing lithofacies, facies association and facies
869 succession of the sequence II. See Figure 2 for explanation of symbols and position of
870 the logs. See Table 1 for facies code. (B) Lithofacies Sp. Planar cross-bedded
871 sandstones. Hummer: 0.3 m. (C) Lithofacies St. superimposed sets of trough cross-
872 bedded sandstones. Hummer: 0.3 m. (D) Mud intraclasts concentrated at the base of
873 cross-bedded set (lithofacies St). Hummer: 0.3 m.

874

875 Figure 6: (A) Sedimentological log showing lithofacies, facies association and facies
876 succession of the sequence III. See Figure 2 for explanation of symbols and position of
877 the logs. See Table 1 for facies code. (B) Lithofacies Gm. Massive conglomerate
878 composed of mudstones and sandstones intraformacional clasts held within a medium
879 to coarse sand matrix. (C) Lithofacies Sp. Planar cross-bedded sandstones. Pencil:
880 0.15 m.

881

882 Figure 7: Onlap of the prodelta to delta front deposits of the Sequence IV over braided
883 fluvial channel sandbodies of the Sequence III. See Figure 2 for position of the
884 sedimentological panel.

885

886 Figure 8: (A) Sedimentological log showing lithofacies, facies association and facies
887 succession of the outcrop 5 (sequence IV). See Figure 2 for explanation of symbols
888 and position of the logs. See Table 1 for facies code. (B) Facies succession of the
889 distributary channel and overbank facies association. (C) Heterolithic deposits of the
890 overbank facies association characterized by intercalation of the massive sandstones
891 (Sm) and massive mudstones with mud cracks (Fm). (D) and (E) Coarsening upward
892 facies succession of the prodelta and delta front facies association. Person: 1.6 m.

893

894 Figure 9: (A) Sedimentological log showing lithofacies, facies association and facies
895 succession of the outcrop 1(sequence IV). See Figure 2 for explanation of symbols and
896 position of the logs. See Table 1 for facies code. (B) Outcrop panel showing lateral
897 accretion surface in meandering fluvial channel sandstone bodies.

898

899 Figure 10: Rose diagrams showing cross-bedding dip directions of the prodelta /delta
900 front and distributary channel facies association of the Sequence IV. $n= 105$.

901

902 Figure 11: Depositional models depicting the temporal evolution of the upper jurassic-
903 neocomian rift succession of the Araripe Basin, representing four distinct sequences
904 accumulated during different rift tectonic stages. See text for discussion.

905

906 Figure 11: Continued.

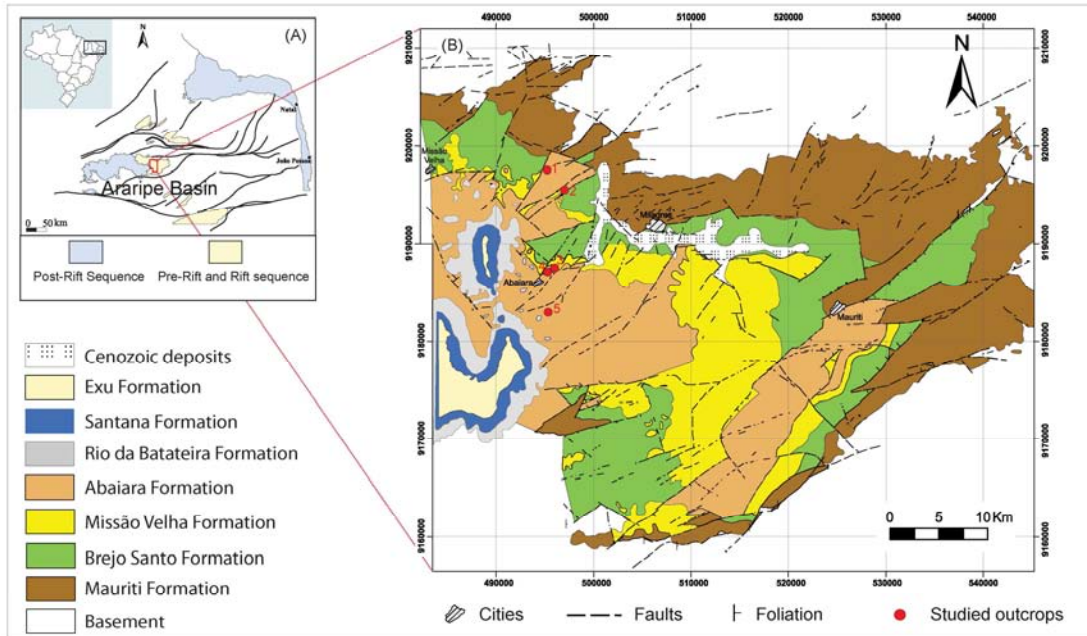
907

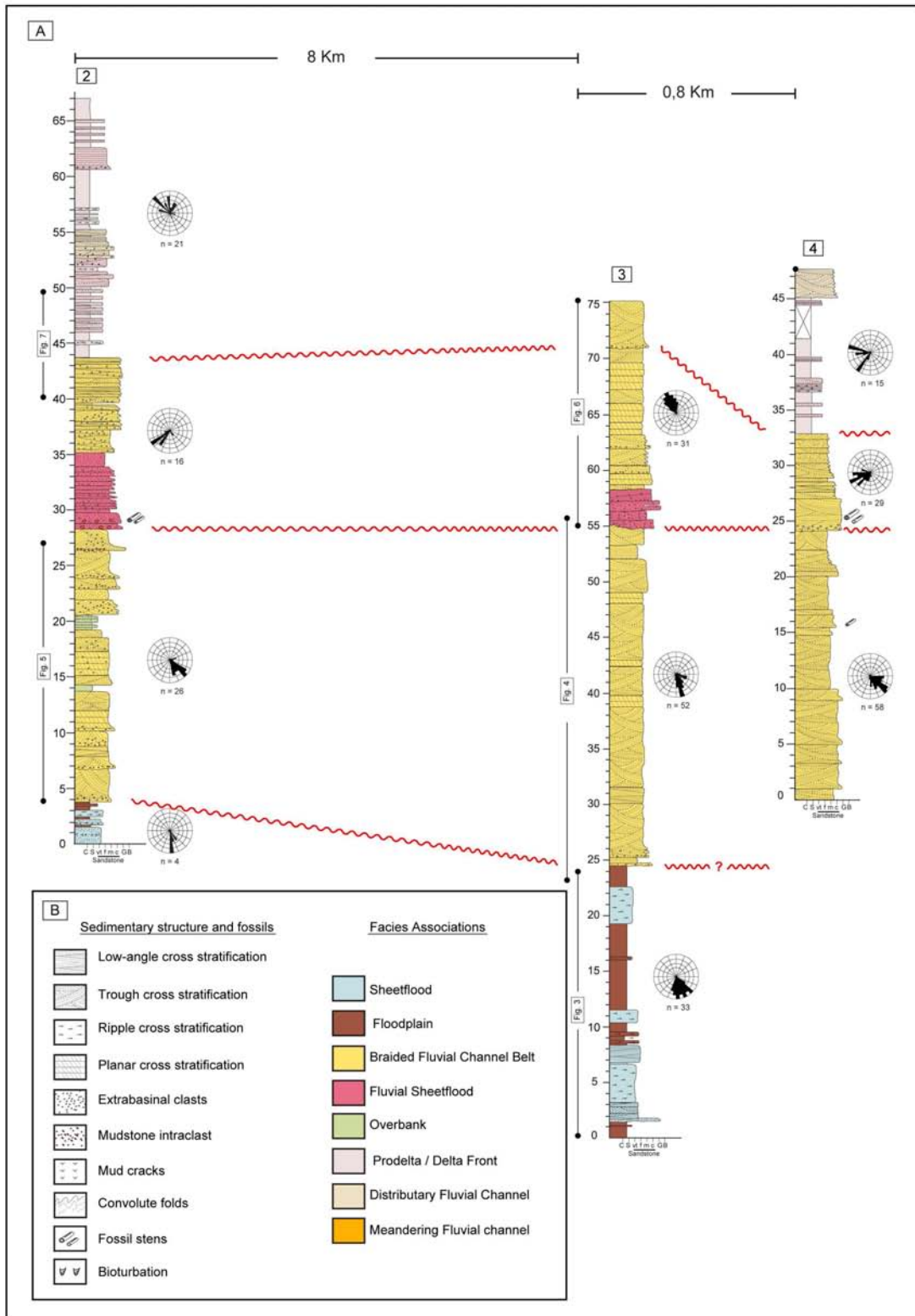
908

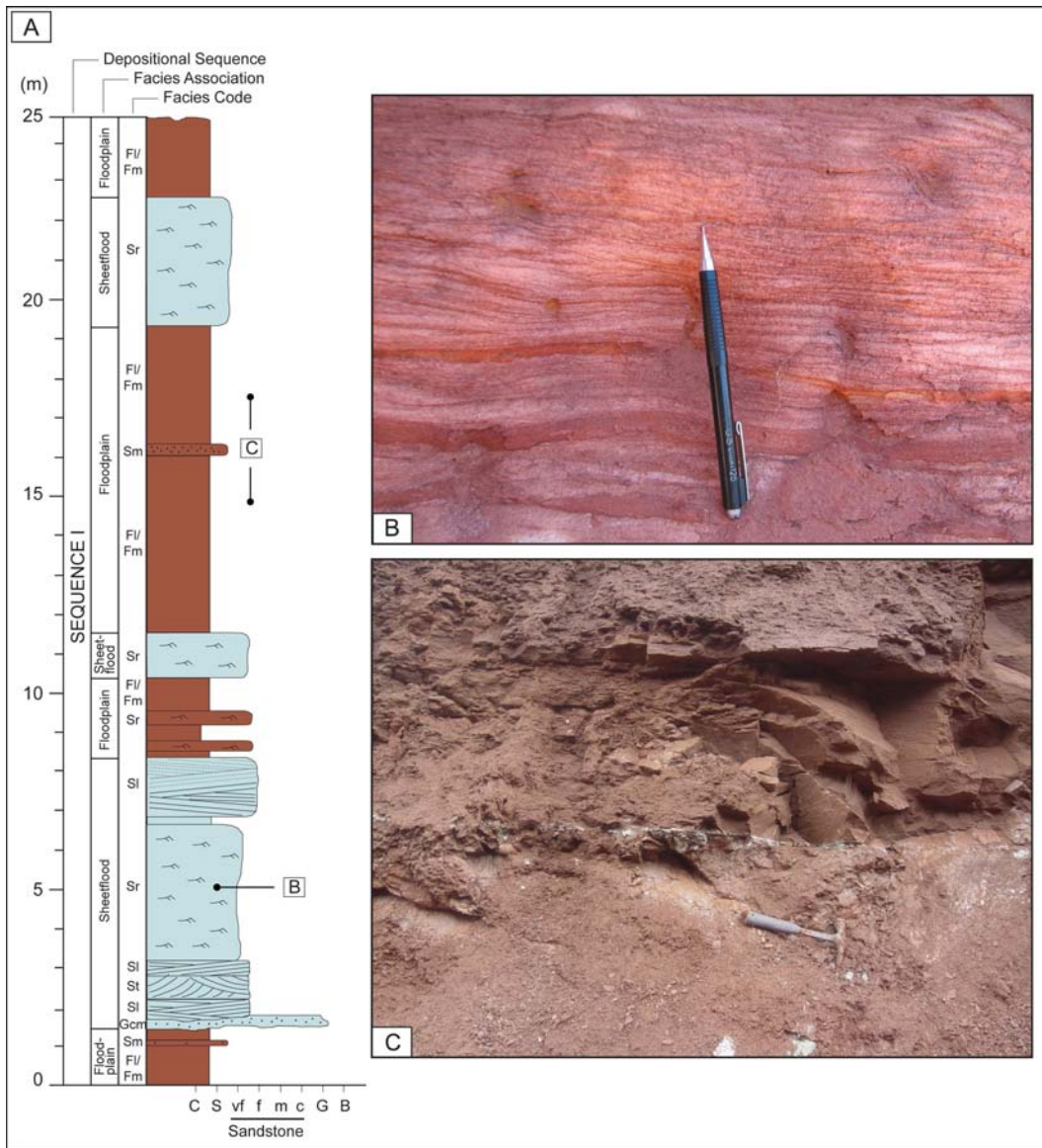
ACCEPTED MANUSCRIPT

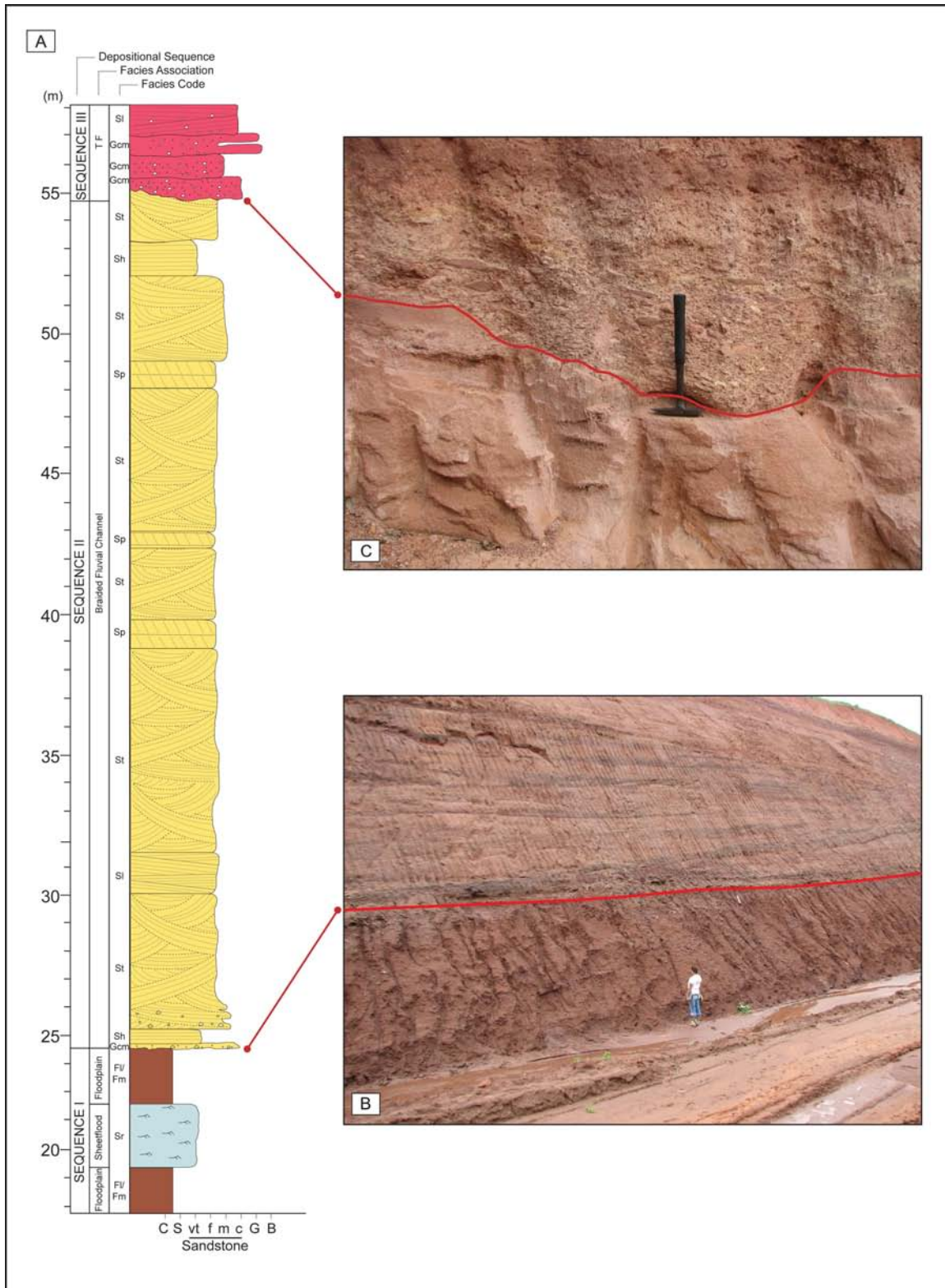
GEOCHRONOLOGY		SEQUENCE STRATIGRAPHY	LITOSTRATIGRAPHY		THIS PAPER
CRETACEOUS	NEO	POS-RIFT SUPERSEQUENCE	ARARIPE GROUP	EXU FORMATION	
	EO			ARARIPINA FORMATION	
				SANTANA FORMATION	
				BARBALHA FORMATION	
		RIFT SUPERSEQUENCE	ABAIARA FORMATION	SEQUENCE IV	
NEO JURASSIC	NEO	PRE-RIFT SUPERSEQUENCE	VALE DO CARIRI GROUP	MISSÃO VELHA FORMATION	SEQUENCE III
					SEQUENCE II
				BREJO SANTO FORMATION	SEQUENCE I
PALEOZOIC		PALEOZOIC SEQUENCE	MUCURI FORMATION		

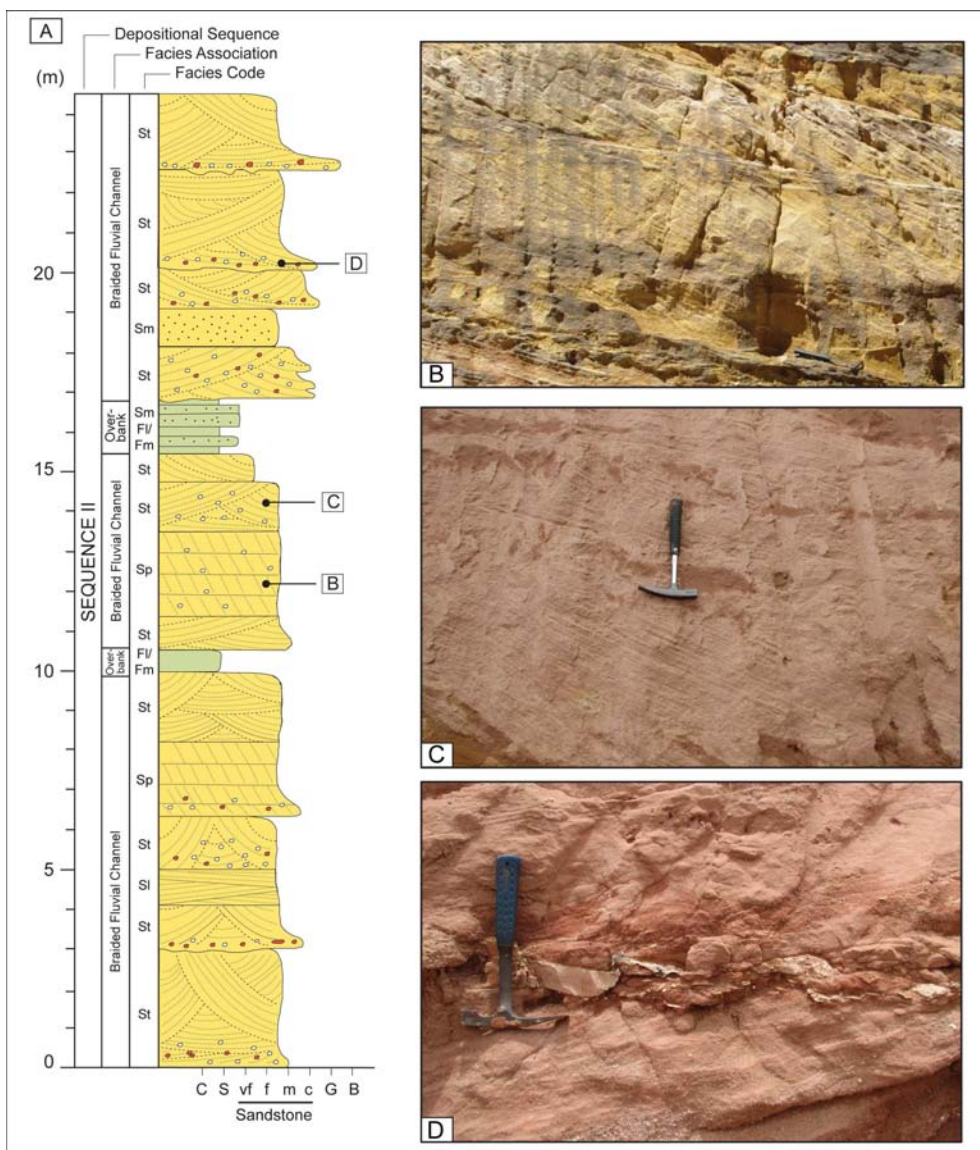
Facies	Description	Interpretation
Gcm	Sandy conglomerate; granule to pebble clasts; massive; intraformacional clasts of mudstones and sandstones; rare extraformacional clasts of granite, gneiss, quartzite.	Pseudoplastic debris flow
Gt	Sandy conglomerate; granule to pebble clasts; extraformacional clasts of granite and quartz; coarse to granular sandstone matrix, vaguely to well stratified; 10 to 40 cm thick sets; trough cross-stratified sets	3-D gravel dunes
Sm	Fine to coarse-grained sandstones; moderated to well sorted; massive; 20 to 40 cm thick beds.	Rapid deposition from heavily sediment-laden flows during waning floods or intense fluidization
St	Fine to coarse-grained sandstones; moderated sorted; rare extraformacional granule and pebble clasts of granite and quartz; 20 cm to 1m thick sets; trough cross-stratification. Sometimes soft sediment deformation.	3-D subaqueous sand dunes (lower flow regime)
Sp	Fine to coarse-grained sandstones; moderated sorted; rare extraformacional granule and pebble clasts of granite and quartz, dispersed or parallel to stratification; 10 to 50cm thick sets; planar cross-stratification. Sometimes soft sediment deformation.	2-D subaqueous sand dunes (lower flow regime)
Sl	Fine to coarse-grained sandstones; moderated sorted; common extraformacional granule and pebble clasts of granite and quartz; cross-stratification dips $<10^0$ with respect to bedding; 20 to 40 cm thick bed .	Washed-out dunes and humpack dunes (transition between subcritical and supercritical flows)
Sl(e)	Fine- to medium-grained sandstones; well sorted with well-rounded and highly spherical grains; low angle cross-lamination composed by inversely graded laminae, up to 10 mm thick.	Subcritical climbing translant strata formed by the migration of wind ripples under conditions of net sedimentation.
Sh	Fine to coarse-grained sandstones; moderated sorted; common extraformacional granule and pebble clasts of granite and quartz; flat parallel lamination; rare parting lineations on bedding plane; 10 to 40 cm thick bed.	Planar bedded deposition under upper plane-bed flow condition
Sr	Fine to coarse-grained sandstones; ripple cross-lamination, supercritical to subcritical climbing angle; 1 to 5 cm thick sets that may form up to 1.5 m thick cosets.	2D- or 3D- ripples (lower flow regime); climbing ripple formation during periods of rapid sedimentation.
Fl	Mudstones to very fine-grained sandstones; flat parallel lamination; rare small-scale ripple cross-lamination (<1 cm).	Suspension fallout with very weak current;
Fm	Mudstone; massive; desiccation cracks; carbonate palaeosols.	Suspension setting over flood plains; later modified by desiccation

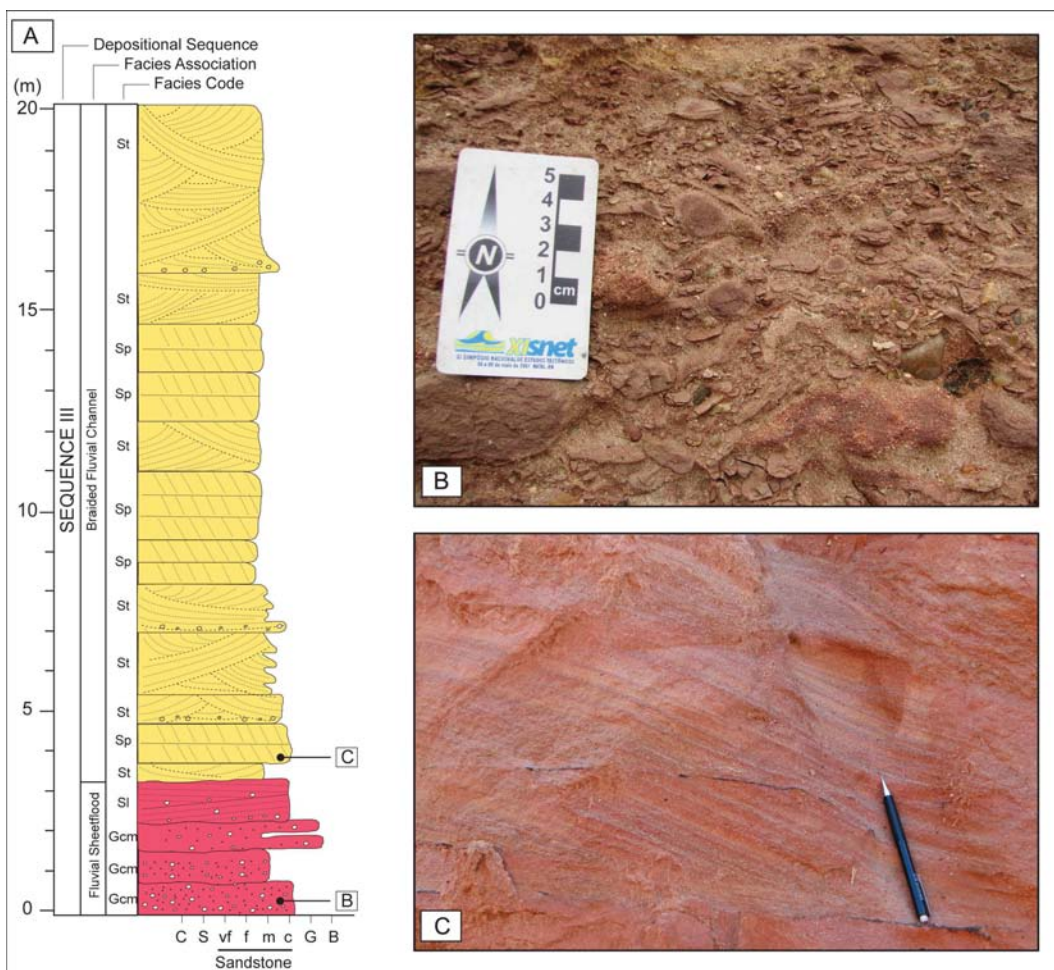


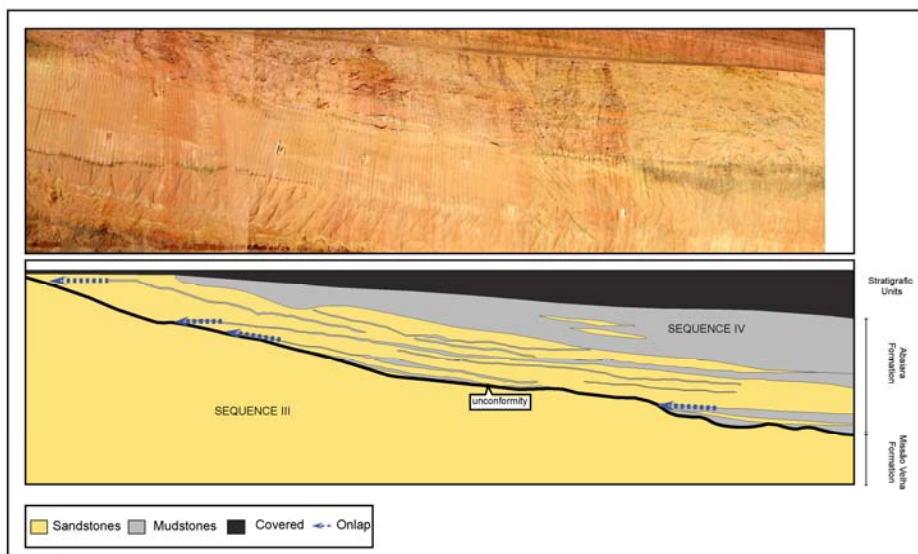


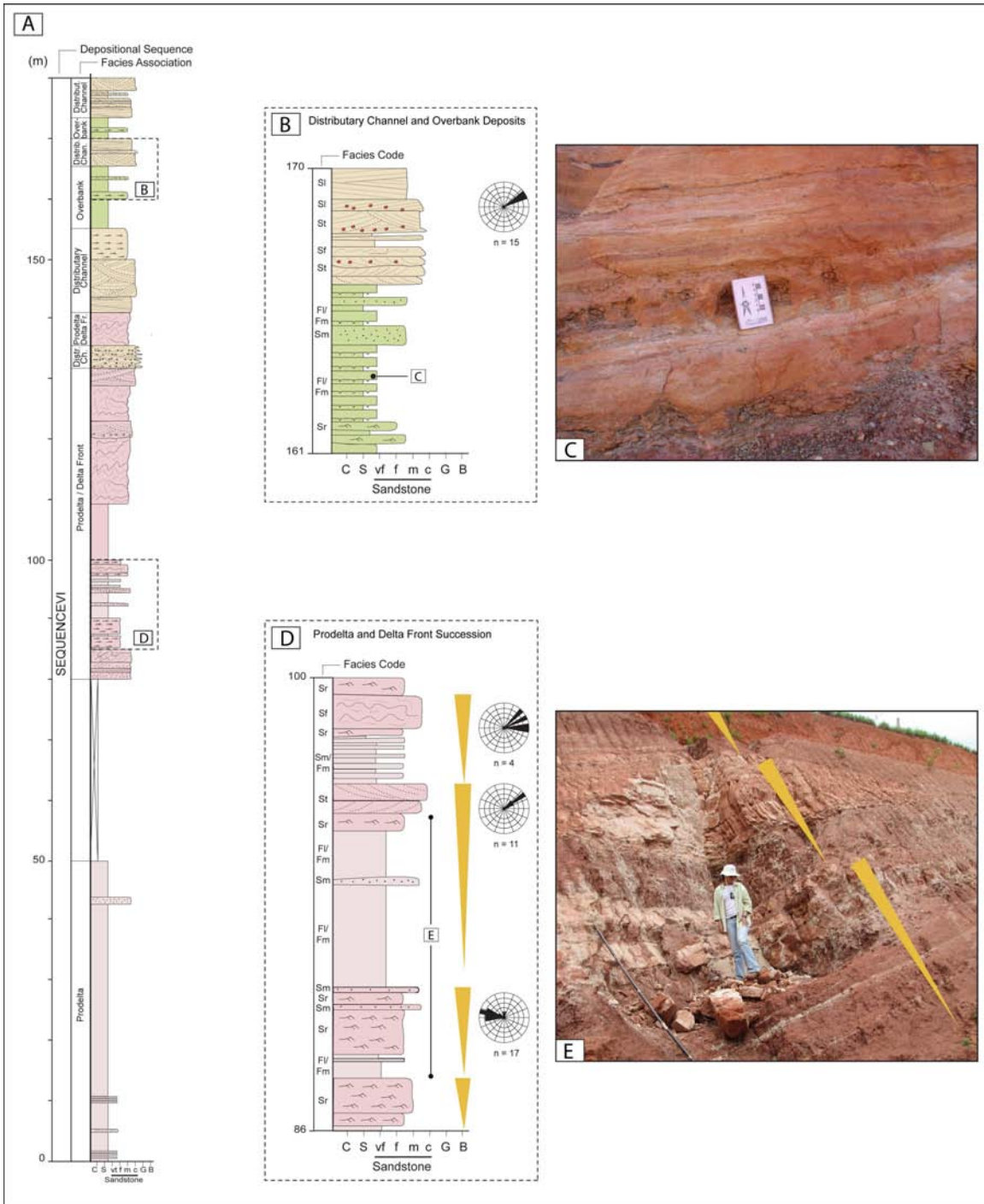


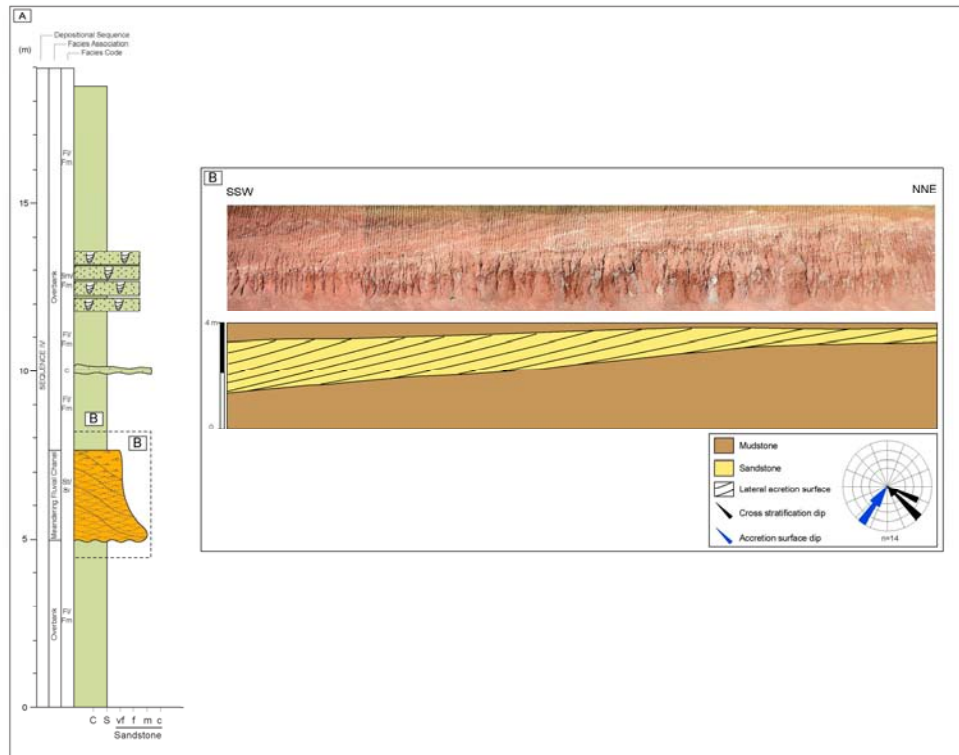




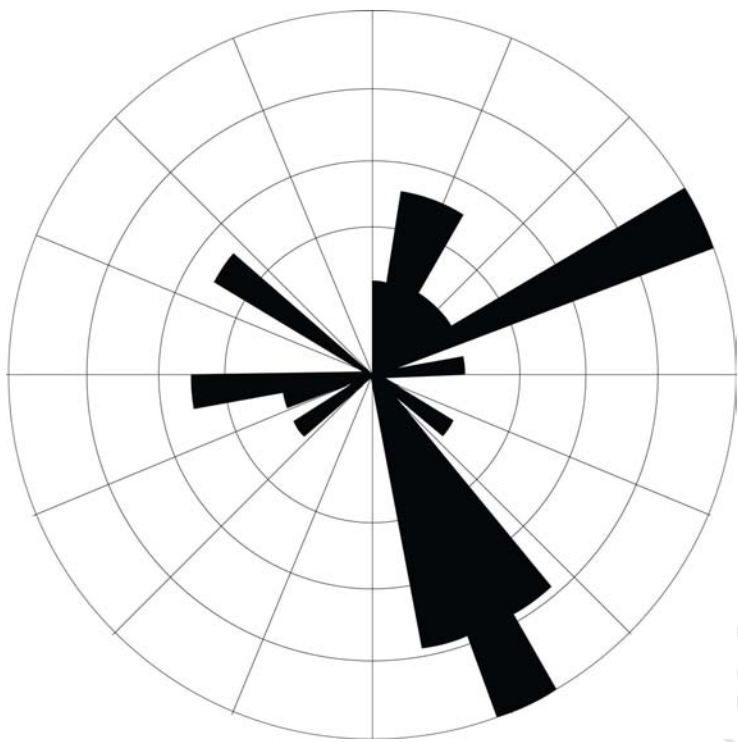




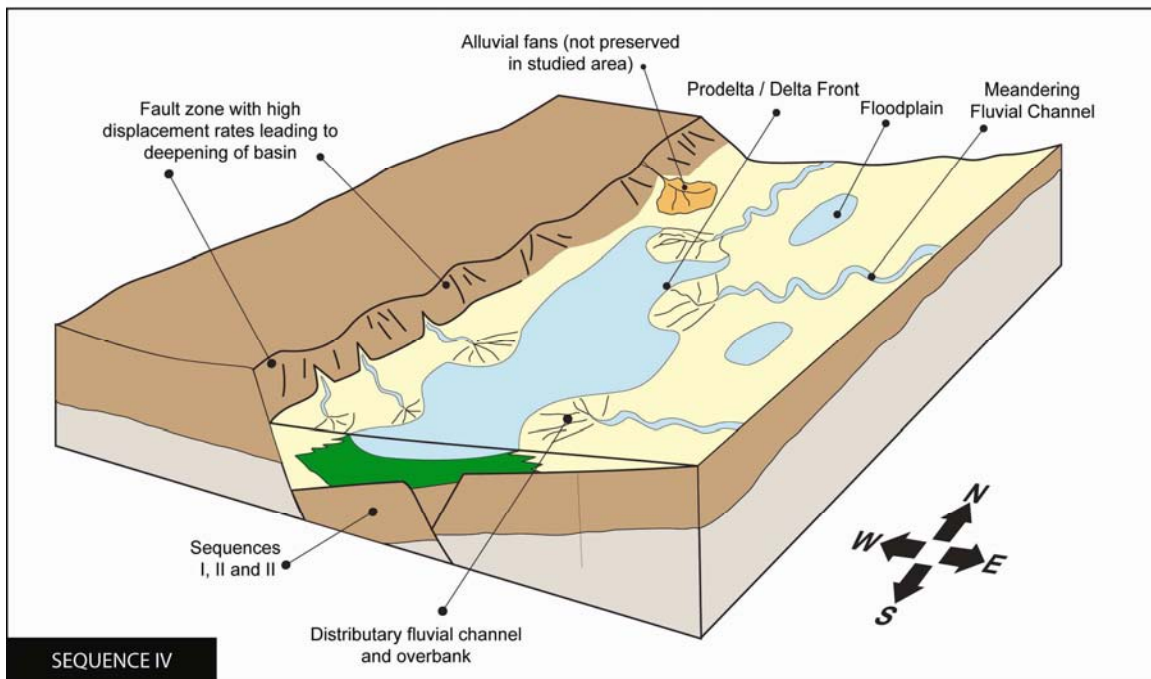
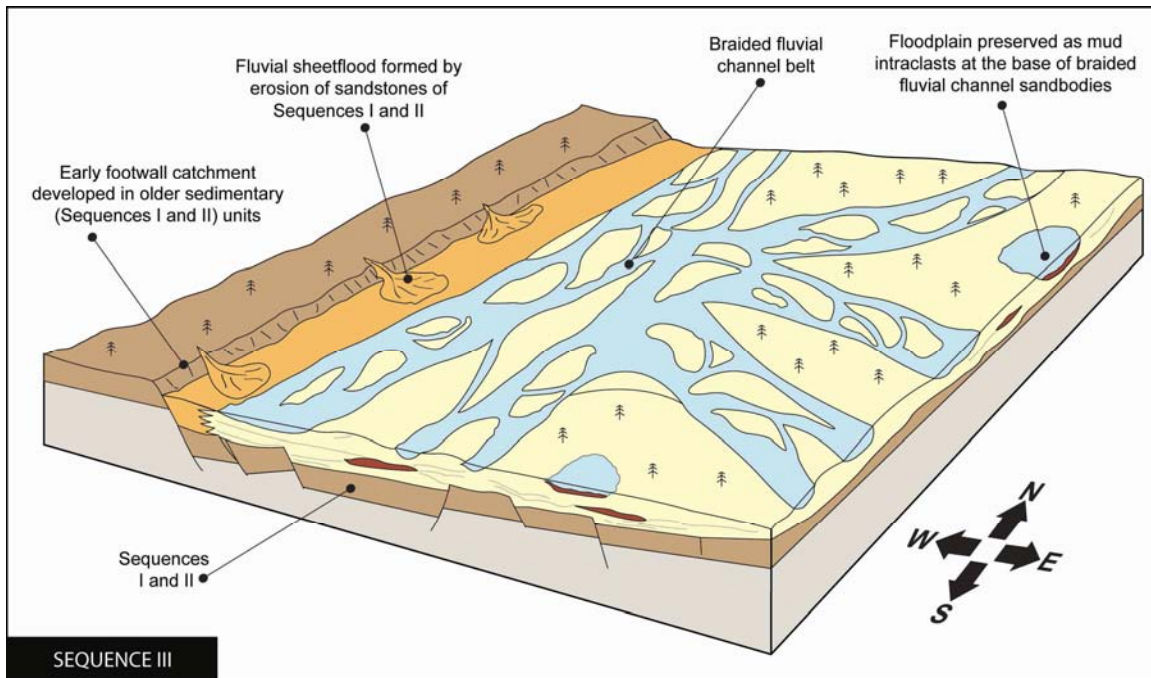


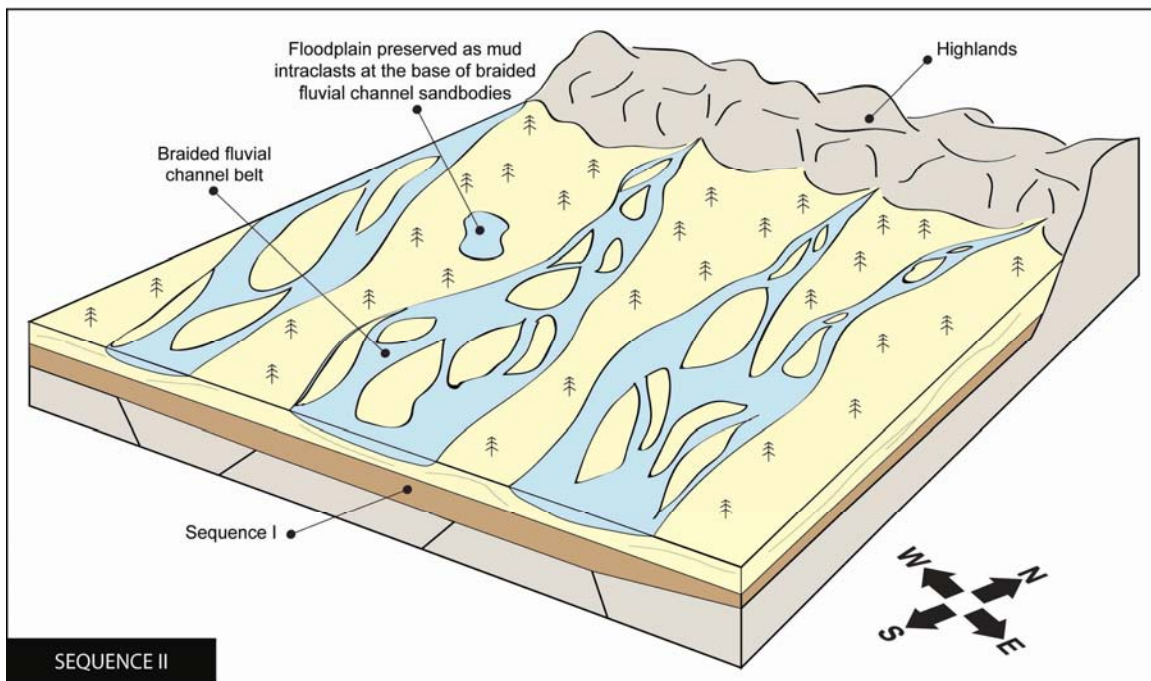
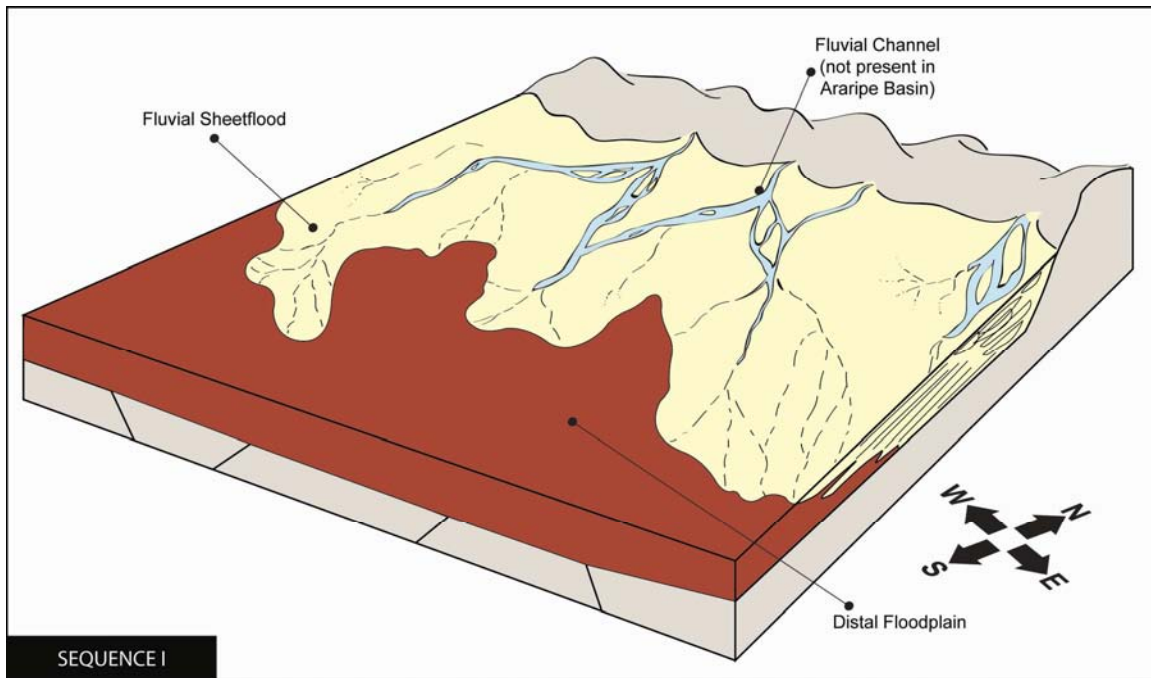


ACCEPTED



ACCEPTED MANUSCRIPT





- Rift section of the Araripe Basin can be subdivided into four depositional sequences.
- These sequences record different evolutionary stages of Araripe Basin.
- Sequences I, II and III represent a record of a larger basin associated to early rift stage.
- Sequence IV was accumulated in well-defined half-graben systems.

ACCEPTED MANUSCRIPT